Journal of Medicinal Chemistry

Article

Structure-Based Design, Synthesis and in vivo Antinociceptive Effects of Selective A1 Adenosine Receptor Agonists#

Riccardo Petrelli, Mirko Scortichini, Carmela Belardo, Serena Boccella, Livio Luongo, Fabio Capone, Sonja Kachler, Patrizia Vita, Fabio Del Bello, Sabatino Maione, Antonio Lavecchia, Karl-Norbert Klotz, and Loredana Cappellacci

J. Med. Chem., **Just Accepted Manuscript** • DOI: 10.1021/acs.jmedchem.7b01399 • Publication Date (Web): 19 Dec 2017

ACS Publications

Journal of Medicinal Chemistry is published by the American Chemical Society. 1155 Sixteenth Street N.W., Washington, DC 20036

Structure-Based Design, Synthesis and *in vivo* Antinociceptive Effects of Selective A_1 Adenosine Receptor Agonists[#]

Riccardo Petrelli,[1] Mirko Scortichini,[1] Carmela Belardo,[2] Serena Boccella,[2] Livio Luongo,[2] Fabio Capone,[3] Sonja Kachler,[4] Patrizia Vita,[1] Fabio Del Bello,[1] Sabatino Maione,[2] Antonio Lavecchia,[3*] Karl-Norbert Klotz,[4] and Loredana Cappellacci[1*]

[1]*School of Pharmacy, Medicinal Chemistry Unit, University of Camerino, 62032 Camerino, Italy*
[2]*Section of Pharmacology "L. Donatelli", Department of Experimental Medicine, University of Campania "L. Vanvitelli", 80138 Naples, Italy*
[3]*Department of Pharmacy,"Drug Discovery" Laboratory, University of Naples Federico II, 80131 Naples, Italy*
[4]*Institut für Pharmakologie and Toxikologie, Universität Würzburg, D-97078 Würzburg, Germany*

Keywords: A_1 adenosine receptor agonists, antinociceptive activity, formalin test, N^6-substituted-5′-chloro-5′-deoxy-adenosine derivatives, N^6-substituted-5′-pyrazolyl-adenosine derivatives.

ABSTRACT

Our previous work discovered that combining the appropriate 5′- and N^6-substitution in adenosine derivatives leads to highly selective human A_1 adenosine receptor (hA_1AR) agonists or highly potent dual hA_1AR agonists and hA_3AR antagonists. In order to explore novel dual adenosine receptor ligands, a series of N^6-substituted-5′-pyrazolyl-adenosine and 2-chloro-adenosine derivatives were synthesized and assayed *in vitro* at all ARs. The N^6-(±)-*endo*-norbornyl derivative **12** was the most potent and selective at A_1AR and effective as an analgesic in formalin test in mice, but none of the 5′-pyrazolyl series compounds showed a dual behaviour at hA_1 and hA_3AR. Molecular modeling studies rationalized the structure-activity relationships and the selectivity profiles of the new series of A_1AR agonists. Interestingly, an unexpected inverted binding mode of the N^6-tetrahydrofuranyl derivative **14** was hypothesized to explain its low affinity at A_1AR.

INTRODUCTION

Adenosine is an endogenous purine nucleoside that modulates a variety of physiological functions as a result of its activation of specific G protein-coupled receptors defined as A_1, A_{2A}, A_{2B}, and A_3 adenosine receptors (ARs).[1]

The A_1 adenosine receptor (A_1AR) is the best characterized adenosine receptor subtype. Selective A_1AR agonists mediate neuro- and cardioprotective effects, reduce lipolysis in adipose tissue, and intraocular pressure in glaucoma.[2,3] The A_1AR is abundantly expressed in spinal cord and other neuronal tissue, and its activation produces pain-relieving effects in a number of preclinical animal models.[4-6]

Several selective A_1AR agonists have been developed as analgesics, e.g. *N*-cyclohexyl-2'-*O*-methyladenosine (SDZ WAG 994)[7], *N*-[(1*S*,2*S*)-2-hydroxycyclopentyl]adenosine (GR79236)[8], (*2S,3S,4R,5R*)-2-(5-tert-butyl-1,3,4-oxadiazol-2-yl)-5-(6-(4-chloro-2-fluoroanilino)purin-9-

yl)tetrahydrofuran-3,4-diol (GW493838)[9]. However, clinical trials of these nucleosides have been discontinued, possibly due to their inability to penetrate CNS sufficiently to cause a substantial effect.[10] Moreover, high doses may produce severe side effects, especially in the cardiovascular system (bradycardia and hypotension).[10]

N^6-substituted- and/or sugar-modified adenosine derivatives have been the subject of numerous publications on the structure activity relationship (SAR) at ARs.[11-17] The nature of the substituents at the N^6- and 5′-positions of adenosine derivatives has a major influence on AR affinity, selectivity and efficacy. Many N^6-substituted-5′-modified adenosine derivatives turned out to be A_1AR agonists,[17] others were found to be A_1AR partial agonists,[13,18] while others behaved as dual human (h) A_1AR agonists and A_3AR antagonists.[16]

Our recent works demonstrated that the substitution of OH at the 5′-position of N^6-substituted adenosine derivatives with a chlorine atom is not only well tolerated by the hA_1AR but even improves the A_1AR selectivity and affinity. 5′-Chloro-5′-deoxy-N^6-(±)-*endo*-norbornyl-adenosine (5′Cl5′d-(±)-ENBA, **3**) turned out to be potent and the most selective human and mouse (m) A_1AR agonist *vs* A_3AR[14,19] with analgesic effects in a mouse model of neuropathic pain.[20] Interestingly, at analgesic doses, **3** did not lower blood pressure or locomotor activity in mice.[20,21] Moreover, it was found to reduce the dyskinesia caused by L-DOPA in a mouse model of Parkinson desease (PD).[22]

A_3AR is the last of the adenosine receptor subtypes to be cloned. A_3AR agonists are in advanced clinical studies in the treatment of hepatocellular carcinoma, psoriasis and rheumatoid arthritis.[23,24] Recently, Salvemini and colleagues have reported that highly selective A_3AR agonists produce antinociceptive effects at both central and peripheral levels without cardiovascular side effects and, unlike opioids, without inherent reward.[6,25,26] Moreover, the authors proved that A_3AR agonists modified pathological but not normal protective nociception.[26]

Also, A_3AR antagonists are potentially useful in the treatment of various diseases such as glaucoma, [3,27] asthma, septic shock and other conditions.[28,29]

Modification at the ribose moiety of adenosine derivatives was found to modulate both the affinity and efficacy at the A_1 and A_3 ARs. While 5′-chloro-5′-deoxy-N^6-substituted adenosine derivatives turned out to be potent hA_1AR agonists that were highly selective *vs* hA_3AR[14] and mA_3AR,[19] 5′-*C*-ethyl-tetrazol-2-yl-N^6-substituted adenosine derivatives were found to be highly potent dual hA_1AR agonists and hA_3AR antagonists.[16] Surprisingly, 5′-*C*-ethyl-tetrazol-2-yl-N^6-substituted adenosine derivatives proved to be agonists at the rat (r) A_3AR that were endowed with strong analgesic activity in a formalin test in mice.[30] Therefore, combining the appropriate 5′-modification and N^6-substitution in adenosine derivatives leads to dual A_1AR and A_3AR ligands having different profiles of affinity and efficacy in human and other species. These dual acting ligands might have the advantages of being a single molecule and associated pharmacokinetics, but activating different signaling pathways, both leading to beneficial effects in the treatment of various diseases, e.g. pain (dual A_1 and A_3 AR agonists), glaucoma and epilepsy (dual A_1 agonist and A_3 AR antagonist). For this reason, in order to explore novel combinations of 5′-modification and N^6-substitution leading to dual A_1 and A_3AR ligands, a series of 5′-deoxy-5′-pyrazolyl-adenosine and 2-chloroadenosine derivatives (compounds **9-16**) was synthesized and evaluated for affinity and selectivity at all cloned hAR subtypes. Some 2,5′-bis-pyrazolyl-5′-deoxy-adenosine derivatives (compounds **17-20**) and the intermediate 5′-chloro-5′-deoxy-N^6-substituted adenosine derivatives, compounds **5-8**, were also assayed at all AR subtypes. The most active compounds of the series were tested for their *in vivo* analgesic activity in mice. A molecular modeling study rationalized the observed binding data of this series of 5′,N^6-disubstituted adenosine derivatives.

RESULTS AND DISCUSSION

Chemistry. The novel compounds **5-20** were synthesized according to the methods reported in Schemes 1 and 2. The synthesis of compounds **5-8** is outlined in Scheme 1. Treatment of 6-chloro-[31] or 2,6-dichloro-9*H*-(2,3,5-tri-*O*-acetyl-*β*-D-ribofuranosyl)-purine[32] (**21** and **22**, respectively) with 4-chloro-2-fluoroaniline in the presence of triethylamine in absolute ethanol, followed by sugar deblocking with methanolic ammonia, afforded compounds **25** and **26** in good yields. N^6-[(*R*)-3-Tetrahydrofuranyl]adenosine (Tecadenoson, **23**), 2-chloro-tecadenoson (**24**) and the corresponding 2′,3′-isopropylidene derivatives **27** and **28** respectively, were synthesized as previously reported.[18,33,34]

Compounds **25** and **26** were then converted into their corresponding 2′,3′-isopropylidene derivatives **29** and **30** using camphorsulfonic acid and 2,2-dimethoxypropane in acetone. Chlorination of **27**-**30** to the corresponding 5′-chloro derivatives **31**-**34** was performed by treatment with a mixture of thionyl chloride, pyridine, and acetonitrile. Finally, deisopropylidenation of **31**-**34** with 70% formic acid at 40 °C furnished the desired compounds **5**-**8**. The reference compounds 5′-chloro-5′-deoxy-N^6-cyclopentyl-adenosine (5′-Cl-CPA, **1**), 2-chloro-5′-chloro-5′-deoxy-N^6-cyclopentyl-adenosine (5′-Cl-CCPA, **2**), **3**, and 2-chloro-5′-chloro-5′-deoxy-N^6-(±)-*endo*-norbornyl-adenosine (2-Cl-5′Cl5′d-(±)-ENBA, **4**) were synthesized as previously reported.[14] As outlined in Scheme 2, direct substitution of 5′-chloro-5′-deoxy-adenosine derivatives **1**-**8** with hydrazine monohydrate and subsequent condensation of the resulting intermediates **35**-**46** with acetylacetone in ethanol afforded the target 5′-pyrazolyl and 2,5′-dipyrazolyl N^6-substituted adenosine derivatives **9**-**20**.

Binding Affinity.

Compounds **9**-**20** were tested in radioligand binding assays for affinity at the human recombinant ARs, stably transfected into Chinese hamster ovary (CHO) cells, utilizing radioligand binding assays (A_1, A_{2A}, and A_3) (Table 1, see also Supporting Information, Figure S1).[35] Based on our

previous results with **3**,[14,20-22] the intermediate 5′-chloro-5′-deoxy-adenosine derivatives **5-8** were also assayed at all AR subtypes.

As shown in Table 1, 5′-deoxy-5′-(3,5-dimethyl)-pyrazolyl-N^6-substituted adenosine derivatives **9-16** showed hA_1AR affinity from the low nanomolar to half micromolar (4.35-491 nM), and some of them were highly selective *vs* A_{2A} and A_3ARs. 5′-Deoxy-5′-pyrazolyl-N^6-(±)-*endo*-norborn-2-yl-2-chloroadenosine (**12**) was the most potent and selective analogue (A_1AR K_i = 4.35 nM, selectivity A_{2A}/A_1 = 2168 fold and A_3/A_1 = 333 fold, Table 2). As previously reported in the 5′-chloro-5′-deoxy-N^6-substituted adenosine derivatives series,[14] in the 5′-pyrazolyl one, the N^6-(±)-*endo*-norborn-2-yl substitution furnished the highest affinity at A_1AR. The N^6-tetrahydrofuranyl substitution was not well tolerated, with compounds **13** and **14** (A_1AR K_i = 491 and 438 nM, respectively) being 100-fold less potent than compound **12**. The 2-fluoro-4-chlorophenyl substitution (compounds **15** and **16**) was also less well tolerated (A_1AR K_i = 158 and 139 nM, respectively) than the *endo*-norbornyl one (compounds **11** and **12**, A_1AR K_i = 25.6 and 4.35 nM, respectively), though to a lesser extent. The substitution with a pyrazolyl group at the 2 position in 5′-deoxy-5′-pyrazolyl-N^6-substituted adenosine derivatives (**17-20**) was well tolerated at A_1AR. K_i values of compounds **17-20** ranged from 8.02 to 91.4 nM at A_1AR with N^6-cyclopentyl-2,5′-bis-pyrazolyl-5′-deoxy-adenosine (**17**) being the most potent and selective hA_1AR agonist among the 2,6-bis-pyrazolyl- derivatives. However, the most potent compounds at hA_1AR turned out to be the intermediate 5′-chloro-5′-deoxy-adenosine derivatives **5-8** (K_i values ranging from 1.87 to 11.2 nM). Compound **5** was found the most selective A_1 *vs* A_3AR of the series (A_3AR/A_1AR = 635 fold).

At hA_3AR, the 5′-deoxy-5′-pyrazolyl-, and the 5′-chloro-5′-deoxy-derivatives (**9-20** and **5-8**, respectively) showed from moderate to very low affinity (K_i values ranging from 0.136 to 5.64 μM). It is interesting to note that even though compound **16** displayed moderate affinity (K_i at both A_1 and A_3 ARs = 139 nM), it turned out to be a dual hA_1 and hA_3 ligand that was highly selective *vs* A_{2A} and A_{2B} ARs (A_{2A}/A_1 = > 720, A_{2B}/A_1 = > 430).

Adenylyl Cyclase Activity.

Due to the lack of a useful high-affinity radioligand for A_{2B}AR, all novel compounds were tested in a functional A_{2B}AR assay and the EC_{50} values are reported in Table 1 (see also Supporting Information, Figure S3). None of the compounds showed particularly high potency. The most potent compound **7** showed an EC_{50} comparable to NECA.[35]

Selected compounds were additionally tested for their functional effects at hA_1AR, and hA_3AR by measuring modulation of adenylyl cyclase activity. The ability of these compounds to inhibit forskolin-stimulated cAMP production via the hA_1AR and the hA_3AR was studied in comparison with the full A_1 agonist CCPA[36] and the non-selective agonist NECA,[37] respectively (Supporting Information, Figures S2 and S4). Compounds were considered to be antagonists if they fully reversed (>85%) the NECA-mediated inhibition of adenylyl cyclase activity.

As expected, all tested compounds were found to be agonists at hA_1ARs, whereas they were antagonists at the hA_3AR subtype. EC_{50} values at A_1 and/or IC_{50} values at A_3AR of selected compounds were also determined (Table 3). The most potent compounds at A_1AR were the 5′-chloro-5′-deoxy-adenosine derivatives **6** and **7**, showing EC_{50} values of 54.2 and 56 nM, respectively (Table 3). Among the 5′-deoxy-5′-pyrazolyl-adenosine derivatives, compound **12** showed the best EC_{50} value at hA_1AR (EC_{50} =134 nM), while compound **16** showed the best IC_{50} value at hA_3AR (IC_{50} = 701 nM).

Molecular Modeling.

The 5′-deoxy-5′-pyrazolyl-N^6-(±)-*endo*-norborn-2-yl adenosine compound **12** (A_1, K_i = 4.35 nM) exhibited excellent binding affinity, and the N^6-(*R*)-3-tetrahydrofuranyl and N^6-2-fluoro-4-chloro-phenyl analogues **14** (A_1, K_i = 438 nM) and **16** (A_1, K_i = 139 nM) showed, respectively, ≈100-fold and ≈32-fold less binding affinity at the hA_1AR. In addition, the presence of a chlorine atom in the β-D-ribofuranose ring in **6** led to a substantial increase in its binding affinity at the hA_1AR with a K_i of 3.50 nM. In view of the observed variations in the hA_1AR binding affinities among these

compounds, molecular docking experiments were carried out by the means of the GOLD 5.4.1 program[39] in combination with the ChemPLP[40] scoring function (rescoring with ChemScore).[41] Although two crystal structures are available now for the hA1AR,[42,43] both represent the inactive conformation of the receptor bound to covalent and non-covalent antagonists. Comparison of agonist-bound and inactive conformations of the A_{2A}AR crystal structures revealed several conformational changes needed for receptor activation, especially within the ligand binding region. These conformational changes include a tightening of hydrophilic residues in TM3, TM5 and TM7 around the ribose moiety, resulting in a significant contraction in the volume of the binding site.[44] Based on these observations, docking was performed considering the homology model of the hA_1AR, built using the recently solved agonist-bound hA_{2A}AR crystal structure (PDB ID: 3QAK) as a template.[45]

The docking poses of **6** (CHEMscore fitness = 20.22 kJ/mol), **12** (CHEMscore fitness = 20.90 kJ/mol) and **16** (CHEMscore fitness = 20.11 kJ/mol) highlighted the crucial anchoring interactions with the binding site of hA_1AR that are expected to be common among all the A_1AR agonists (Figure 1). A strong H-bond interaction was observed between the carboxamide group of $N254^{6.55}$ (using standard notation[46] and the exocyclic N^6 amino group and the N^7 atom of the adenine ring of three ligands. The C2-chlorine atom was within H-bonding distance from the NH_2 group of $N70^{2.65}$ side chain. The adenine core was anchored inside the binding site by a π–π stacking interaction with F171 (extracellular loop 2) and strong hydrophobic contacts with $L250^{6.51}$ and $I274^{7.39}$.

Moreover, the 3′- and 2′-OH groups of **6** were located in proximity to $T277^{7.42}$ and $H278^{7.43}$, respectively, and could form H-bonds with these residues. In contrast, the ribose ring of compounds **12** and **16**, as a result of the bulky and rigid 3,5-dimethyl-pyrazole substituent at the 5′ position, was subjected to a slight rotation about the N9-C1′ bond, thereby allowing only the 3′-OH group to form a H-bond with $H278^{7.43}$. In particular, while **6**, which has a less bulky chlorine atom in 5′, presented a glycosyl torsion angle χ (defined by O-C1'-N9-C4 in Figure 2) clearly

indicative of an *anti*-conformation (χ = -152.4°), the same parameter for compounds **12** and **16** showed values still within the *anti*-conformation range but with a slight shift toward an *anti*/*syn* intermediate state (χ = 165.4, χ = -164.3, respectively). Figure 2 illustrates the comparison of the binding modes of compounds **6** and **12**, highlighting the different orientation of the sugar moiety in the adenosine derivatives.

The 5′-(3,5-dimethyl)-pyrazole moiety of **12** (Figure 1B) and **16** (Figure 1C) was locked in the cavity by a H-bond with T91$^{3.36}$, with the threonine side chain acting as H-bond donator, while the hydrophobic methyl groups attached at 2 and 5 positions of pyrazole were held by favorable vdW interactions with residues L88$^{3.33}$, Q92$^{3.37}$, M180$^{5.38}$, N184$^{5.42}$, V189$^{5.47}$, W247$^{6.48}$, L250$^{6.51}$, and H251$^{6.52}$.

The 5′ substituent of **6** consists of a chloromethyl group. A high flexibility of the Cl atom in the 5′ subpocket of A_1AR appeared in the docking results for chloromethyl agonist **6**, with different orientations of the Cl atom. Nevertheless, in 145 out of 200 cases GOLD found one recurring solution in which the 5′-Cl atom of **6** was engaged in a H-bond interaction with H251$^{6.52}$ (Figure 1A). Interestingly, the importance of this interaction in agonist recognition has been recently demonstrated in the adenosine-bound A_{2A}AR structure,[47] where the interaction between the 5′-OH group of the cocrystallized adenosine and the residues H250$^{6.52}$ and N181$^{5.42}$ is mediated by a structured water molecule (wat2017 in the PDB entry 2YDO).[47]

Based on docking results, differences can be observed in the interactions formed by the ribose moiety of compounds **6**, **12** and **16**; in fact, compounds **12** and **16** formed only two of the three H-bonds predicted for binding of the full agonist **6** (EC_{50} = 54.2 nM). In particular, compounds **12** and **16** (Figure 1B,C) established H-bonds with H278$^{7.43}$, and T91$^{3.36}$ and not with T277$^{7.42}$. However, their ability to bridge between TM3 and TM7 likely correlates with the capacity to induce the conformational changes required for receptor activation, such as an inward movement of TM7.

In contrast with **6**, **12** and **16**, derivative **14** (CHEMscore fitness = 15.35 kJ/mol) appeared to have an inverted binding mode and did not maintain some key conserved interactions for binding (Figure 1D). The less bulky N^6-tetrahydrofuranyl substituent, mimicking the ribose moiety of the natural agonist adenosine, occupied a region close to ribose binding pocket but did not mimic the H-bonding interactions of the 3′- and 2′-OH groups with T277$^{7.42}$ and H278$^{7.43}$, respectively. This result explains why appending a tetrahydrofuranyl group at the N^6 position dramatically decreases the A_1AR binding affinity.

Furthermore, the different nature of the substituents at the N^6 position of the adenine ring of **6**, **12** and **16** could influence the selectivity and the efficacy of the agonists at three hAR subtypes. The N^6 groups in the docking poses of the studied agonists accommodated in a pocket, which was located between TM6 and TM7 and delimited by residues L253$^{6.54}$, T257$^{6.58}$, T270$^{7.35}$, M177$^{5.38}$, and at the bottom by L250$^{6.51}$. Also note of the hA_1AR subtype accommodates more dramatic differences compared to both hA_{2A}AR and hA_3AR among residues controlling the upper region of the binding site, and this could affect the orientation and the interactions of the N^6-substituents for each receptor subtype.[42] For example, position 6.54 in A_1AR consists of a nonconserved bulky and hydrophobic leucine residue, while a smaller isoleucine is present in the other AR subtypes. The corresponding residues of T270$^{7.35}$ in A_1AR are the bulky Met270$^{7.35}$ in A_{2A}AR and L264$^{7.35}$ in A_3AR. Another residue located in the N^6 subpocket and involved in the anchoring of the N^6 substituent of the A_1AR agonists, but nonconserved among the adenosine receptors, is the T257$^{6.58}$, which becomes a bulky leucine in hA_3AR.

The variation of the affinity and potency of this series of 5′-pyrazolyl adenosine analogues at the A_1AR indicates that the N^6 substituent could greatly affect these factors, in some cases counterbalancing for the lack of H-bonding interactions in the ribose region. In particular, the pocket at the upper part of the hA_1AR was found to have a shape more suitable to accommodate a N^6-norbornyl (compound **12**) or N^6-tetrahydrofuranyl (compound **6**) substituent. On the other hand, compound **16**, which has a more flexible and extended 2-fluoro-4-chloro-phenyl group at N^6

position, exhibits poor steric complementarity to the pocket as compared to the norbornyl or tetrahydrofuranyl groups and consequently has lower affinity at the A_1AR.

Antinociceptive Effect.

Selected compounds endowed with high hA_1AR affinity and selectivity (**5, 6** and **12**) were evaluated *in vivo* in mice by performing the formalin test.

Formalin injection induces a biphasic stereotypical nocifensive behavior.[48] Nociceptive responses are divided into an early, short lasting first phase (0-7 min) caused by a primary afferent discharge produced by the stimulus, followed by a quiescent period and then a second, prolonged phase (15-60 min) of tonic pain. Systemic administration of **5** (2 mg/kg, i.p.), 10 min before formalin, slightly reduced only the early phase of the formalin test, while the highest dose of **5** used (4 mg/kg) reduced both the early and the late phases of the formalin test. This effect was prevented by 8-cyclopentyl-1,3-dipropyl-xanthine (DPCPX, **50**)[49] (1 mg/kg, i.p.), a selective A_1AR antagonist (Figure 3).

Systemic administration of **6** (0.25, 0.5 and 2 mg/kg, i.p.), 10 min before formalin, reduced the late nociceptive behavior induced by formalin in a dose-dependent manner ($P < 0.005$). The highest dose of **6** used (2 mg/kg) significantly reduced only the late phase of the formalin test, and this effect was prevented by **50** (1 mg/kg, i.p.) (Figure 4).

Systemic administration of **12** (1, 2 and 4 mg/kg, i.p.), 10 min before formalin, reduced the late nociceptive behavior induced by formalin in a dose-dependent manner ($P < 0.05$) (Figure 5).

CONCLUSION

In conclusion, this study confirmed that N^6-substituted 5′-chloro-5′-deoxy-adenosine and 2-chloro-adenosine derivatives are potent and selective A_1AR agonists potentially useful in the treatment of pain. The substitution of a 5′-chlorine atom with a (3,5-dimethyl)-pyrazolyl moiety reduces both the affinity and the selectivity at A_1AR with respect to the corresponding 5′-chloro-5′-deoxy-

derivatives. As previously reported for **3**, the N^6-(±)-*endo*-norbornyl substituent allowed to obtain compound **12**, the most potent and selective A_1AR agonist in the series of 5′-deoxy-5′-pyrazolyl derivatives. Moreover, a molecular modeling study rationalized the unexpected low affinity at A_1AR of compounds **13** and **14**.

While a 5′-*C*-tetrazolyl- moiety in adenosine derivatives was highly tolerated at both hA_1 and hA_3AR subtypes leading to potent dual acting A_1 and A_3AR ligands, the 5′-(3,5-dimethyl)-pyrazolyl moiety was tolerated at A_1AR but not at A_3AR.

In conclusion, in this work we discovered a new series of N^6,5′-disubstituted-adenosine and 2-chloro-adenosine derivatives as potent hA_1AR agonists useful in the treatment of pain.

EXPERIMENTAL SECTION

Chemical Synthesis. Materials and Instrumentation. All reagents and solvents were purchased from Sigma-Aldrich Chemical Co, were analytical grade and were used as received. Thin layer chromatography (TLC) was run on silica gel 60 F254 plates; column chromatography was run on silica gel 60 (70−230 mesh, Merck and 200−400 mesh, Merck). Preparative thin layer chromatography was run on silica gel GF (20 cm × 20 cm, 1000 μm, Analtech). The final compounds were characterized by ^{1}H NMR, ^{13}C NMR, MS, and elemental analyses. ^{1}H NMR and ^{13}C NMR spectra were recorded on 400 MHz NMR spectrometer (Varian Mercury AS400 instrument). The chemical shift values are expressed in δ values (ppm), and coupling constants (J) are in hertz; tetramethylsilane (TMS) was used as an internal standard. Proton chemical data are reported as follows: chemical shift, multiplicity (s = singlet, d = doublet, dd = doublet of doublets, pd = pseudo doublet, t = triplet, dt = doublet of triplets, q = quartet, dq = doublet of quartets, m = multiplet, brs = broad singlet) coupling constant (s), integration. The presence of all exchangeable protons was confirmed by addition of D_2O. The purity of final compounds was checked using an Agilent 1100 series HPLC equipped with Gemini-NX 5μm C-18 100Å 250 x 4.6 mm column.

Mobile phase consisted of a mixture of water/methanol (95:5) at a flow rate of 1 mL/min. Peaks were detected by UV adsorption with a diode array detector (DAD) at 230, 254, and 280 nm. All derivatives tested for biological activity showed ≥96% purity by HPLC analysis (Area % purity was detected at 210 nm or 254 nm). Mass spectra were recorded on an HP 1100 series instrument. All measurements were performed in the positive ion mode using atmospheric pressure electrospray ionization (API-ESI). Elemental analyses (C, H, and N) were determined on ThermoFisher Scientific FLASH 2000 CHNS analyzer and are within 0.4% of theoretical values. Biological assays: [^{3}H]CCPA was purchased from Amersham/GE Healthcare (58 Ci/mmol – 2.15 TBq/mmol; Purity 98.4%); [^{3}H]NECA was purchased from American Radiolabeled Chemicals Inc. (25 Ci/mmol – 0.93 TBq/mmol, Purity 99%); [^{3}H]HEMADO was purchased from Tocris (24 Ci/mmol – 0.89 TBq/mmol, Purity > 97%). DPCPX (**50**) was purchased from Tocris (Bristol, UK).

General Procedure for the Synthesis of Compounds 5-8.

Compounds **31**-**34** (1 equiv) were treated with HCOOH 70% in water (10 mL), and the mixture was stirred at 40 °C for the time reported below. The solvent was evaporated to dryness, and the residues were coevaporated several times with CH_3OH and then purified by column chromatography.

***N*^{6}-(*R*)-3-Tetrahydrofuranyl-9*H*-(5-chloro-5-deoxy-β-D-ribofuranosyl)adenine (5).**

The title compound was synthesized from **31** (150 mg, 0.380 mmol). Chromatography on a silica gel column ($CHCl_3$-MeOH, 97:3) gave **5** as a white foam (68 mg, 50% yield). ^{1}HNMR (DMSO-d_6): δ 1.95-2.23 (2m, 2H, tetrahydrofuranyl), 3.60 (dd, *J* = 4.51, 8.80 Hz, 1H, tetrahydrofuranyl), 3.72 (q, *J* = 7.7 Hz, 1H, tetrahydrofuranyl), 3.80-3.96 (m, 4H, tetrahydrofuranyl, H-5′), 4.08 (q, *J* = 5.32 Hz, 1H, H-4′), 4.20 (q, *J* = 4.71 Hz, 1H, H-3′), 4.58-4.71 (m, 1H, C*H*NH), 4.74 (q, *J* = 5.31 Hz, 1H, H-2′), 5.46 (d, *J* = 5.10 Hz, 1H, OH), 5.60 (d, *J* = 6.0 Hz, 1H, OH), 5.92 (d, *J* = 5.5 Hz,

1H, H-1′), 7.98 (brs, 1H, NH), 8.22 (brs, 1H, H-2), 8.38 (s, 1H, H-8). ^{13}C NMR (DMSO-d_6): 43.88, 52.35, 53.95, 67.55 (2C), 71.82, 72.89, 86.07, 96.21, 119.32, 140.21, 148.88, 152.24, 154.56. MS (API-ESI): *m/z* 356.8 $[M+H]^+$. Anal. calcd. For ($C_{14}H_{18}ClN_5O_4$) C, 47.26; H, 5.10; N, 19.68; Found: C, 47.24; H, 5.12; N, 19.67.

2-Chloro-N^6-(*R*)-3-tetrahydrofuranyl-9*H*-(5-chloro-5-deoxy-β-D-ribofuranosyl)adenine (6).

The title compound was synthesized from **32** (150 mg, 0.350 mmol). Chromatography on a silica gel column ($CHCl_3$-MeOH, 98:3) gave **6** as a white foam (128 mg, 95% yield). ^{1}HNMR (DMSO-d_6): δ 1.86-2.29 (m, 2H, tetrahydrofuranyl), 3.54-3.83 (m, 4H, tetrahydrofuranyl), 3.86-3.96 (m, 2H, H-5′), 4.33-4.39 (m, 1H, H-4′), 4.62 (brs, 1H, *CH*NH), 5.11 (q, *J* = 3.2 Hz, 1H, H-3′), 5.41 (dd, *J* = 2.99, 6.21 Hz, 1H, H-2′), 6.21 (s, 1H, H-1′), 8.38 (s, 1H, H-8), 8.62 (brs, 1H, NH). ^{13}C NMR (DMSO-d_6): 43.91, 52.27, 53.85, 67.47 (2C), 71.73, 72.92, 86.12, 96.25, 119.15, 140.29, 148.93, 153.12, 154.71. MS (API-ESI): *m/z* 391.3 $[M+H]^+$. Anal. calcd. for($C_{14}H_{17}Cl_2N_5O_4$) C, 43.09; H, 4.39; N, 17.95; Found: C, 43.07; H, 4.38; N, 17.96.

N^6-(4-Chloro-2-fluorophenyl)amino-9*H*-(5-chloro-5-deoxy-β-D-ribofuranosyl)adenine (7).

The title compound was synthesized from **33** (130 mg, 0.286 mmol). Chromatography on a silica gel column ($CHCl_3$-MeOH, 98:2) gave **7** as a white foam (81 mg, 68% yield). ^{1}HNMR (DMSO-d_6): δ 3.85 (dd, *J* = 6.41, 11.54 Hz, 1H, H-5′), 3.95 (dd, *J* = 5.13, 11.54 Hz, 1H, H-5′), 4.11 (q, *J* = 5.34 Hz, 1H, H-4′), 4.21 (q, *J* = 4.49 Hz, 1H, H-3′), 4.78 (q, *J* = 5.56 Hz, 1H, H-2′), 5.48 (d, *J* = 5.13 Hz, 1H, OH), 5.62 (d, *J* = 5.98 Hz, 1H, OH), 5.96 (d, *J* = 5.98 Hz, 1H, H-1′), 7.31 (dd, *J* = 2.13, 8.98 Hz, 1H, arom.), 7.52 (dd, *J* = 2.35, 10.47 Hz, 1H, arom.), 7.62 (t, *J* = 8.55 Hz , 1H, arom.), 8.31 (s, 1H, H-2), 8.52 (s, 1H, H-8), 9.68 (s, 1H, NH). ^{13}C NMR (DMSO-d_6): 45.22, 71.76, 73.41, 84.33, 88.03, 117.41, 119.45, 124.82, 129.65, 131.13, 142.13, 158.44, 153.11,

153.95, 152.06, 157.97. MS (API-ESI): *m/z* 415.218. Anal. calcd. for ($C_{16}H_{14}Cl_2FN_5O_3$) C, 46.39; H, 3.41; N, 16.91; Found: C, 46.37; H, 3.43; N, 16.92.

2-Chloro-N^6-(4-chloro-2-fluorophenyl)amino)-9*H*-(5-chloro-5-deoxy-β-D-ribofuranosyl) adenine (8).

The title compound was synthesized from **34** (120 mg, 0.245 mmol). Chromatography on a silica gel column ($CHCl_3$-MeOH, 98:2) gave **8** as a white foam (79 mg, 72% yield). ^{1}HNMR (DMSO-d_6): δ 3.85 (dd, *J* = 6.41, 11.54 Hz, 1H, H-5′), 3.94 (dd, *J* = 5.13, 11.54 Hz, 1H, H-5′), 4.12 (q, *J* = 5.55 Hz, 1H, H-4′), 4.19 (q, *J* = 4.91 Hz, 1H, H-3′), 4.67 (q, *J* = 5.55 Hz, 1H, H-2′), 5.51 (d, *J* = 5.13 Hz, 1H, OH), 5.65 (d, *J* = 5.98 Hz, 1H, OH), 5.89 (d, *J* = 5.55 Hz, 1H, H-1′), 7.32 (d, *J* = 8.55 Hz,1H, arom.), 7.51-7.63 (m, 2H, arom.), 8.49 (s, 1H, H-8), 10.21 (s, 1H, NH). ^{13}C NMR (DMSO-d_6): 45.37, 71.88, 73.54, 84.65, 88.15, 117.44, 119.71, 125.42, 129.68, 131.37, 142.03, 148.78, 153.39, 154.05, 156.08, 158.57. MS (API-ESI): *m/z* 449.66 $[M+H]^+$. Anal. calcd. for ($C_{16}H_{13}Cl_3FN_5O_3$) C, 42.83; H, 2.92; N, 15.61; Found: C, 42.85; H, 2.91; N, 15.63.

General Procedure for the Synthesis of Compounds 9-20.

A solution of compounds **1-8** (1 equiv) in EtOH/H_2O (1:1 v/v) and hydrazine monohydrate (10 equiv) was allowed to stir at room temperature for 24 h. The reaction mixture was then concentrated in vacuo to yield crude compounds **35-46** which were used in the next step directly without purification. To a suspension of **35-46** (1 equiv) in methanol (10 mL) containing 3 drops of glacial acetic acid was added acetylacetone (2 equiv) and the mixture was heated at 80 °C for the time reported below. After completion, the reaction mixture was evaporated to dryness and the residue purified by column chromatography.

N^6-Cyclopentyl-9*H*-(5-(3,5-dimethyl-1*H*-pyrazol-1-yl)-5-deoxy-*β*-D-ribofuranosyl)adenine (9).

The title compound was synthesized from **1** (130 mg, 0.367 mmol, reaction time 5 h) following the general procedure described above. Chromatography on silica gel column ($CHCl_3$–MeOH, 95:5) gave **9** as a white solid (53 mg, 35% yield).^{1}HNMR (DMSO-d_6): δ 1.45-1.61 (m, 4H, cyclopentyl), 1.64-1.77 (m, 2H, cyclopentyl), 1.82-1.95 (m, 2H, cyclopentyl), 2.03 (s, 3H, CH_3), 2.07 (s, 3H, CH_3), 4.15-4.22 (m, 2H, H-5′), 4.27 (br s, 1H, H-4′), 4.48 (br s, 1H, C*H*NH), 4.52 (q, *J* = 5.13 Hz, 1H, H-3′), 4.64 (s, 1H,H-2′), 5.33 (d, *J* = 5.13 Hz, 1H, OH), 5.51 (d, *J* = 5.99 Hz, 1H, OH), 5.72 (s, 1H, pyrazoyl), 5.86 (d, *J* = 5.56 Hz, 1H, H-1′), 7.71 (br s, 1H, NH), 8.05 (s, 1H, H-2), 8.2 (br s, 1H, H-8).^{13}C NMR (DMSO-d_6): 11.23, 13.61, 23.86 (2C), 32.53 (2C), 52.83, 56.21, 72.09, 74.22, 84.27, 88.22, 104.91, 119.78, 140.38, 141.31, 147.93, 150.02, 152.48, 154.96 MS (API-ESI): *m/z* 414.48 $[M+H]^+$. Anal. calcd. for ($C_{20}H_{27}N_7O_3$) C, 58.10; H, 6.58; N, 23.71; Found: C, 58.11; H, 6.57; N, 23.72.

2-Chloro-N^6-cyclopentyl-9*H*-(5-(3,5-dimethyl-1*H*-pyrazol-1-yl)-5-deoxy-*β*-D-ribofuranosyl) adenine (10).

The title compound was synthesized from **2** (140 mg, 0.360 mmol, reaction time 5 h) following the general procedure described above. The residue was purified by chromatography on a silica gel column with $CHCl_3$/MeOH (1-5%) as the eluent affording the fast migrating compound **10** as a white solid (66 mg, 41% yield).^{1}H NMR ($CDCl_3$) δ 1.58-1.71 (m, 4H, cyclopentyl), 1.73-1.82 (m, 2H, cyclopentyl), 2.02-2.08 (m, 2H, cyclopentyl), 2.32 (s, 3H, CH_3), 2.71 (s, 3H, CH_3), 3.82 (dq, *J* = 3.52, 11.96 Hz, 2H, H-5′), 4.41 (dd, *J* = 2.99, 5.56 Hz, 1H, H-4′), 4.46-4.54 (m, 2H, H-3′,C*H*NH), 4.57 (t, *J* = 5.77, 1H, H-2′),5.26 (d, *J* = 5.15 Hz, 1H, OH), 5.48 (d, *J* = 5.78 Hz, 1H, OH), 5.96 (br s , 1H, NH), 6.02 (s, 1H, pyrazoyl), 6.38 (d, *J* = 5.13Hz, 1H, H-1′), 8.02 (s,1H. H-8). ^{13}C NMR (DMSO-d_6): 11.21, 13.59, 23.81 (2C), 32.48 (2C), 52.79, 56.28, 72.11, 74.25, 84.32, 88.31, 105.02, 119.81, 140.41, 141.37, 147.98, 150.06, 152.43, 153.11 MS (API-ESI): *m/z* 448.92

[M+H]$^+$. Anal. calcd. for ($C_{20}H_{26}ClN_7O_3$) C, 53.63; H, 5.55; N, 21.89; Found: C, 53.64; H, 5.86; N, 21.88.

N^6-(±)-*endo*-Norbornyl-9*H*-(5-(3,5-dimethyl-1*H*-pyrazol-1-yl)-5-deoxy-*β*-D-ribofuranosyl) adenine (11).

The title compound was synthesized from **3** (135 mg, 0.355 mmol, reaction time 6 h) following the general procedure described above. Chromatography on silica gel column ($CHCl_3$–MeOH, 95:5) gave **11** as a white solid (97 mg, 62 % yield). ^{1}H NMR (DMSO-d_6): δ 1.21-1.32 (m, 3H, norbornyl), 1.42-1.53 (m, 3H, norbornyl), 1.52-1.65 (m, 1H, norbornyl), 1.83-1.96 (m, 1H, norbornyl), 2.02 (s, 3H, CH_3), 2.09 (s, 3H, CH_3), 2.17 (brs, 1H, norbornyl), 2.33 (brs, 1H, norbornyl), 4.11-4.39 (m, 5H, H-3′, H-4′, H-5′, C*H*NH), 4.55 (brs, 1H, H-2′), 5.35 (d, *J* = 5.13Hz, 1H, OH), 5.54 (dd, *J* = 2.99, 5.76 Hz, 1H, OH), 5.72 (s, 1H, pyrazolyl), 5.86 (d, *J* = 5.56, 1H, H-1′), 7.79 (br s, 1H, CHN*H*), 8.08 (s, 1H, H-2), 8.21 (s, 1H, H-8).^{13}C NMR (DMSO-d_6): 11.15, 13.57, 21.94, 29.64, 34.61, 35.77, 36.98, 38.42, 45.32, 52.96, 71.73, 73.46, 84.64, 87.92, 105.29, 119.43, 140.51, 141.75, 148.36, 150.22, 152.43, 155.81 MS (API-ESI): *m/z* 440.52 [M+H]$^+$. Anal. calcd. for ($C_{22}H_{29}N_7O_3$) C, 60.12; H, 6.65; N, 22.31; Found: C, 60.13; H, 6.66; N, 22.32.

2-Chloro-N^6-(±)-*endo*-norbornyl-9*H*-(5-(3,5-dimethyl-1*H*-pyrazol-1-yl)-5-deoxy-*β*-D-ribofuranosyl)adenine (12).

The title compound was synthesized from **4** (140 mg, 0.338 mmol, reaction time 9 h) following the general procedure described above. The residue was purified by chromatography on a silica gel column with $CHCl_3$-MeOH (1-5%) as the eluent affording the fast migrating compound **12** as a white solid (72 mg, 45% yield).^{1}H NMR (DMSO-d_6): δ1.20-1.37 (m, 3H, norbornyl), 1.39-1.51 (m, 3H, norbornyl), 1.57-1.71 (m, 1H, norbornyl), 1.81-1.94 (m, 1H, norbornyl), 2.11 (brs, 1H, norbornyl), 2.18 (s, 3H, CH_3), 2.45 (brs, 1H, norbornyl), 2.49 (s, 3H, CH_3), 3.81-4.24 (m, 4H, H-3′, H-4′, H-5′), 4.31 (brs, 1H, C*H*NH), 4.82 (brs, 1H, H-2′), 5.43 (d, *J* = 4.28 Hz, 1H, OH), 5.58 (s,

1H, pyrazolyl), 5.91 (d, *J* = 5.56 Hz, 1H, OH),), 6.05 (d, *J* = 5.42, 1H, H-1′), 8.17 (br s, 1H, CHN*H*), 8.32 (s, 1H, H-8). ^{13}C NMR (DMSO-d_6): 11.12, 13.53, 21.97, 29.62, 34.63, 35.74, 36.95, 38.46, 45.39, 52.91, 71.89, 73.42, 84.59, 87.95, 105.33, 119.47, 140.47, 141.72, 148.36, 150.25, 153.95, 155.91 MS (API-ESI): *m/z* 474.96 $[M+H]^+$. Anal. calcd. for ($C_{22}H_{28}ClN_7O_3$) C, 55.75; H, 5.95; N, 20.69; Found: C, 55.76; H, 5.96; N, 20.68.

N^6-(*R*)-3-Tetrahydrofuranyl-9*H*-(5-(3,5-dimethyl-1*H*-pyrazol-1-yl)-5-deoxy-*β*-D-ribofuranosyl)adenine (13).

The title compound was synthesized from **5** (125 mg, 0.351 mmol, reaction time 5 h) following the general procedure described above. Chromatography on silica gel column ($CHCl_3$-MeOH, 95:5) gave **13** as a white solid (85 mg, 58 % yield). ^{1}H NMR (DMSO-d_6): δ1.21-1.82 (2m, 2H, tetrahydrofuranyl), 2.16 (s, 3H, CH_3), 2.44 (s, 3H, CH_3), 2.92 (dd, *J* = 4.22, 8.70 Hz, 1H, tetrahydrofuranyl), 3.18 (m, 1H, tetrahydrofuranyl), 3.41-3.52 (m, 4H, tetrahydrofuranyl, H-5′), 4.05 (t, *J* = 6.2Hz, 1H, H-4′), 4.07-4.11 (m, 1H, NHC*H*), 4.26 (t, *J* = 5.34 Hz, 1H, H-3′), 4.42 (s, 1H, H-2′), 5.22 (brs, 1H, OH), 5.38 (d, *J* = 5.98Hz, 1H, OH), 5.82 (s, 1H, pyrazolyl), 6.05 (d, *J* = 4.71 Hz, 1H, H-1′), 7.61 (s, 1H, H-2), 7.83 (brs, 1H, H-8), 8.91 (brs, 1H, NH). ^{13}C NMR (DMSO-d_6): 11.18, 13.49, 52.15, 52.92, 53.27, 67.53 (2C), 71.27, 73.69, 84.38, 87.98, 105.39, 119.72, 140.39, 141.89, 147.72, 149.82, 152.43, 155.81. MS (API-ESI): *m/z* 416.45 $[M+H]^+$. Anal. calcd. for ($C_{19}H_{25}N_7O_4$) C, 54.93; H, 6.07; N, 23.60; Found: C, 54.94; H, 6.06; N, 23.61.

2-Chloro-N^6-(*R*)-3-tetrahydrofuranyl-9*H*-(5-(3,5-dimethyl-1*H*-pyrazol-1-yl)-5-deoxy-*β*-D-ribofuranosyl)adenine (14).

The title compound was synthesized from **6** (110 mg, 0.281 mmol, reaction time 9 h) following the general procedure described above. The residue was purified by chromatography on a silica gel column with $CHCl_3$-MeOH (1-3%) as the eluent affording the fast migrating compound **14** as a white solid (65 mg, 51% yield). ^{1}H NMR (DMSO-d_6): δ 2.05-2.12 (m, 2H, tetrahydrofuranyl),

2.18 (s, 3H, CH_3), 2.42 (s, 3H, CH_3), 3.59-3.81 (2m, 4H, tetrahydrofuranyl, H-5′), 4.06 (m, 1H, H-4′), 4.11-4.22 (m, 3H, tetrahydrofuranyl, H-3′), 4.61-4.68 (m, 1H, NHC*H*), 4.81 (s, 1H, H-2′), 5.48 (d, *J* = 4.21 Hz, 1H, OH), 5.58 (d, *J* = 5.55 Hz, 1H, OH), 5.93 (d, *J* = 5.98 Hz, 1H, H-1′), 6.06 (s, 1H, pyrazolyl), 8.31 (brs, 1H, NH), 8.37 (brs, 1H, H-8). ^{13}C NMR (DMSO-d_6): 11.21, 13.53, 52.21, 52.94, 53.23, 67.59 (2C), 71.31, 73.72, 84.41, 88.01, 105.03, 119.68, 140.31, 141.73, 147.68, 149.91, 153.11, 154.83 MS (API-ESI): *m/z* 450.89 $[M+H]^+$. Anal. calcd. for ($C_{19}H_{24}ClN_7O_4$) C, 50.72; H, 5.38; N, 21.79; Found: C, 50.73; H, 5.37; N, 21.78.

N^6-(4-Chloro-2-fluorophenyl)amino)-9*H*-(5-(3,5-dimethyl-1*H*-pyrazol-1-yl)-5-deoxy-*β*-D-ribofuranosyl)adenine (15).

The title compound was synthesized from **7** (110 mg, 0.265 mmol, reaction time 7 h) following the general procedure described above. Chromatography on silica gel column ($CHCl_3$-MeOH, 96:4) gave **15** as a white solid (52 mg, 41 % yield). ^{1}H NMR (DMSO-d_6): δ 2.03 (s, 3H, CH_3), 2.11 (s, 3H, CH_3), 4.19-4.33 (m, 4H, H-3′, H-4′, H-5′), 4.61 (q, *J* = 5.34 Hz, 1H, H-2′), 5.36 (d, *J* = 5.12 Hz, 1H,OH), 5.55 (d, *J* = 5.98 Hz, 1H, OH), 5.72 (s, 1H, pyrazolyl), 5.93 (d, *J* = 5.56 Hz, 1H, H-1′), 7.31 (dd, *J* = 1.5, 8.33 Hz, 1H, arom.), 7.49 (dd, *J* = 2.56, 10.26 Hz, 1H, arom.), 7.63 (t, *J* = 8.55 Hz, 1H, arom.), 8.26 (s, 1H, H-2), 8.31 (s, 1H, H-8), 9.68 (s, 1H, NH). ^{13}C NMR (DMSO-d_6): 11.28, 13.78, 52.46, 72.09, 73.58, 85.22, 89.22, 105.38, 115.22, 118.37, 124.62, 126.23, 128.79, 130.09, 139.06, 140.64,144.67, 147.84, 148.95, 152.63, 156.64. MS (API-ESI): *m/z* 474.89 $[M+H]^+$. Anal. calcd. for ($C_{21}H_{21}ClFN_7O_3$) C, 53.23; H, 4.47; N, 20.69; Found: C, 53.24; H, 4.46; N, 20.70.

2-Chloro-N^6-(4-chloro-2-fluorophenyl)amino)-9*H*-(5-(3,5-dimethyl-1*H*-pyrazol-1-yl)-5-deoxy-*β*-D-ribofuranosyl) adenine (16).

The title compound was synthesized from **8** (120 mg, 0.267 mmol, reaction time 5 h) following the general procedure described above. The residue was purified by chromatography on a silica

gel column with $CHCl_3$-MeOH (1-5%) as the eluent affording the fast migrating compound **16** as a white solid (84 mg, 62% yield).^{1}H NMR (DMSO-d_6): δ 2.12 (s, 3H, CH_3), 2.19 (s, 3H, CH_3), 3.78-3.95 (m, 1H, H-5′), 4.06-4.18 (2m, 2H, H-4′, H-5′), 4.25 (q, *J* = 7.26 Hz, 1H, H-3′), 4.82 (q, *J* = 5.76 Hz, 1H, H-2′), 5.52 (d, *J* = 5.13 Hz, 1H, OH), 5.61 (d, *J* = 5.98 Hz, 1H, OH), 5.74 (s, 1H, pyrazolyl), 5.96 (d, *J* = 6.26 Hz, 1H, H-1′), 7.32 (dd, *J* = 2.12, 9.83 Hz, 1H, arom.), 7.51-7.58 (m, 2H, arom.), 8.48 (s, 1H, H-8), 10.05 (s, 1H, NH). ^{13}C NMR (DMSO-d_6): 11.31, 13.72, 52.51, 72.11, 73.53, 85.31, 89.41, 105.27, 115.43, 118.51, 124.47, 126.36, 128.85, 130.13, 139.13, 140.82, 144.73, 147.89, 149.02, 153.27, 156.91. MS (API-ESI): m/z 509.33 $[M+H]^+$. Anal. calcd. for ($C_{21}H_{20}Cl_2FN_7O_4$) C, 49.62; H, 3.97; N, 19.29; Found: C, 49.63; H, 3.96; N, 19.30.

2-(3,5-Dimethyl-1*H*-pyrazol-1-yl)-*N*^{6}-cyclopentyl-9*H*-(5-(3,5-dimethyl-1*H*-pyrazol-1-yl)-5-deoxy-*β*-D-ribofuranosyl)adenine (17).

Compound **17** was obtained from the same reaction of compound **10** after chromatography on a silica gel column with $CHCl_3$-MeOH (1-5%) as the slowest migrating compound (white solid, 22 mg, 12% yield). ^{1}H NMR ($CDCl_3$) δ 1.53-1.81 (m, 4H, cyclopentyl), 1.83-2.02 (m, 2H, cyclopentyl), 2.04-2.12 (m, 2H, cyclopentyl), 2.13 (s, 3H, CH_3), 2.24 (s, 3H, CH_3), 2.32 (s, 3H, CH_3), 2.68 (s, 3H, CH_3), 4.06 (brs, 1H, H-4′), 4.35 (brs, 2H, H-5′), 4.45 (q, *J* = 5.22 Hz, 1H, H-3′), 4.48 (brs, 1H, C*H*NH), 4.64 (t, *J* = 5.56, 1H, H-2′), 5.33 (d, *J* = 5.11 Hz, 1H, OH), 5.51 (d, *J* = 5.65 Hz, 1H, OH), 5.83 (brs, 2H, pyrazolyl, N*H*CH), 6.02 (s, 1H, pyrazolyl), 6.31 (brs, 1H, H-1′), 7.42 (s, 1H, H-8). ^{13}C NMR (DMSO-d_6): 11.21, 12.38, 13.55 (2C), 23.86 (2C), 32.51 (2C), 52.83, 56.31, 72.26, 74.32, 84.29, 88.36, 104.87, 105.25, 119.59, 140.71, 141.63 (2C), 148.12 (2C), 149.86, 152.22, 154.72. MS (API-ESI): *m/z* 508.59 $[M+H]^+$. Anal. calcd. for ($C_{25}H_{33}N_9O_3$) C, 59.16; H, 6.55; N, 24.84; Found: C, 59.15; H, 6.56; N, 24.85.

2-(3,5-Dimethyl-1*H*-pyrazol-1-yl)-*N*^{6}-(±)-*endo*-norbornyl-9*H*-(5-(3,5-dimethyl-1*H*-pyrazol-1-yl)-5-deoxy-*β*-D-ribofuranosyl) adenine (18).

Compound **18** was obtained from the same reaction of compound **12** after chromatography on a silica gel column with $CHCl_3$-MeOH (1-5%) as the slowest migrating compound (white solid, 39 mg, 22% yield).^{1}H NMR (DMSO-d_6): δ1.19-1.31 (m, 3H, norbornyl), 1.39-1.44 (m, 3H, norbornyl), 1.52-1.67 (m, 1H, norbornyl), 1.81-1.94 (m, 1H, norbornyl), 2.02 (brs, 6H, CH_3), 2.11 (brs, 6H, CH_3), 2.21 (brs, 1H, norbornyl), 2.49 (brs, 1H, norbornyl), 4.11-4.41 (m, 5H, H-3′, H-4′, H-5′,C*H*NH) 4.57 (brs, 1H, H-2′), 5.37 (d, *J* = 5.25 Hz, 1H, OH), 5.52 (d, *J* = 5.45 Hz, 1H, OH), 5.72 (s, 1H, pyrazolyl), 5.88 (s, 1H, pyrazolyl), 6.03 (s, 1H, H-1′), 8.05 (brs, 1H, CHN*H*), 8.09 (s, 1H, H-8). ^{13}C NMR (DMSO-d_6): 11.18, 12.33, 13.45 (2C), 22.08, 29.33, 34.52, 35.82, 36.34, 38.55, 45.22, 53.01, 71.77, 73.82, 84.67, 87.78, 104.96, 105.34, 119.61, 140.68, 141.58 (2C), 148.23 (2C), 149.91, 152.37, 154.77. MS (API-ESI): *m/z* 534.63 $[M+H]^+$. Anal. calcd. for ($C_{27}H_{35}N_9O_3$) C, 60.77; H, 6.61; N, 23.62; Found: C, 60.76; H, 6.62; N, 23.61.

2-(3,5-Dimethyl-1*H*-pyrazol-1-yl)-*N*^{6}-(*R*)-3-tetrahydrofuranyl-9*H*-(5-(3,5-dimethyl-1*H*-pyrazol-1-yl)-5-deoxy-*β*-D-ribofuranosyl) adenine (19).

Compound **19** was obtained from the same reaction of compound **14** after chromatography on a silica gel column with $CHCl_3$-MeOH (1-3%) as the slowest migrating compound (white solid, 29 mg, 20% yield).^{1}H NMR ($CDCl_3$) δ 1.91-2.03 (m, 2H, tetrahydrofuranyl), 2.11 (s, 3H, CH_3), 2.23 (s, 3H, CH_3), 2.29 (s, 3H, CH_3), 2.51-2.63 (m, 1H, tetrahydrofuranyl), 2.67 (s, 3H, CH_3), 3.81-4.03 (m, 4H, tetrahydrofuranyl, H-5′), 4.11 (m, 1H, tetrahydrofuranyl), 4.33 (s, 1H, H-4′), 4.45 (m, 1H, H-3′), 4.71 (t, *J* = 5.40 Hz, 1H, H-2′), 4.77-4.83 (m, 1H, NHC*H*), 5.85 (brs, 1H, OH), 6.02 (brs, 1H, OH), 6.19 (brs, 2H, pyrazolyl), 6.32 (s, 1H, H-1′), 7.55 (brs, 1H, CHN*H*), 8.03 (s, 1H, H-8). ^{13}C NMR (DMSO-d_6): 11.23, 12.34, 13.58 (2C), 52.26, 53.03, 53.28, 67.62 (2C), 71.31, 73.78, 84.48, 88.18, 104.92, 105.22, 119.73, 140.52, 141.77 (2C), 147.79 (2C), 149.96, 152.06, 154.89. MS (API-ESI): *m/z* 510.57 $[M+H]^+$. Anal. calcd. for ($C_{24}H_{31}N_9O_4$) C, 56.57; H, 6.13; N, 24.74; Found: C, 56.56; H, 6.12; N, 24.75.

2-(3,5-Dimethyl-1*H*-pyrazol-1-yl)-*N*^{6}-(4-chloro-2-fluorophenyl)amino)-9*H*-(5-(3,5-dimethyl-1*H*-pyrazol-1-yl)-5-deoxy-*β*-D-ribofuranosyl) adenine (20).

Compound **20** was obtained from the same reaction of compound **16** after chromatography on a silica gel column with $CHCl_3$-MeOH (1-5%) as the slowest migrating compound (white solid, 27 mg, 18% yield).^{1}H NMR (DMSO-d_6): δ 2.12 (s, 3H, CH_3), 2.21 (s, 3H, CH_3), 2.27 (s, 3H, CH_3), 2.48 (s, 3H, CH_3), 4.11-4.39 (m, 4H, H-3′, H-4′, H-5′), 4.58-4.71 (m, 1H, H-2′), 5.28 (d, *J* = 5.32 Hz, 1H, OH), 5.62 (d, *J* = 5.78 Hz, 1H, OH), 5.83 (s, 1H, pyrazolyl), 5.96 (s, 1H, pyrazolyl), 6.11 (d, *J* = 5.45 Hz, 1H, H-1′), 7.09-7.16 (m, 2H, arom.), 7.61-7.72 (m, 1H, arom.), 8.27 (s, 1H, H-8), 9.36 (s, 1H, NH). ^{13}C NMR (DMSO-d_6): 11.32, 12.39, 13.78 (2C), 52.57, 72.19, 73.58, 85.43, 89.52, 104.93, 105.32, 115.22, 119.02, 124.49, 126.42, 128.74, 130.13, 139.22, 140.68 (2C), 144.76, 147.78 (2C), 149.32, 152.93, 157.08. MS (API-ESI): *m/z* 569.02 $[M+H]^+$. Anal. calcd. for ($C_{26}H_{27}ClFN_9O_3$) C, 54.98; H, 4.79; N, 22.19; Found: C, 54.99; H, 4.77; N, 22.18.

General procedure for the *N*^{6}-Amination of 21 and 22 into compounds 25 and 26.

To a stirred solution of 6-chloro-9*H*-(2,3,5-*O*-acetyl-*β*-D-ribofuranosyl)purine (**21**)[31] or 2,6-dichloro-9*H*-(2,3,5-*O*-acetyl-D-ribofuranosyl)purine (**22**)[32] (1 equiv) in absolute ethanol (20 mL), 4-chloro-2-fluoroaniline (1.6 equiv) was added. The reaction mixture was refluxed for the time reported below and concentrated in vacuo. The residue was dissolved in methanolic ammonia (10 mL) and stirred at room temperature overnight. The solution was evaporated to dryness and the residue was purified by chromatography on a silica gel column.

***N*^{6}-(4-Chloro-2-fluorophenyl)amino-9*H*-(*β*-D-ribofuranosyl)adenine (25).**

Reaction of **21** (300 mg, 0.726 mmol) with 4-chloro-2-fluoroaniline (169.1 mg, 129 μL, 1.16 mmol) for 6 h followed by deprotection gave **25**, which was purified by chromatography on a silica gel column ($CHCl_3$-MeOH, 99:1) as a white solid (201 mg, 70% yield).^{1}HNMR (DMSO-

d_6): δ 3.52-3.77 (m, 2H, H-5′), 3.95 (q, *J* = 3.71 Hz, 1H, H-4′), 4.15 (q, *J* = 4.7 Hz, 1H, H-3′), 4.6 (q, *J* = 5.99 Hz, 1H, H-2′), 5.21 (d, *J* = 4.7 Hz, 1H, OH), 5.25 (q, *J* = 4.91 Hz, 1H, OH), 5.48 (d, *J* = 6.42 Hz, 1H, OH), 5.94 (d, *J* = 5.98 Hz, 1H, H-1′), 7.31 (dd, *J* = 1.28, 8.55 Hz, 1H, arom.), 7.53 (dd, *J* = 2.09, 10.26 Hz, 1H, arom.), 7.62 (t, *J* = 8.55 Hz, 1H, arom.), 8.32 (s, 1H, H-2), 8.51 (s, 1H, H-8), 9.71 (br s, 1H, NH). ^{13}C NMR (DMSO-d_6): 61.77, 70.96, 74.33, 86.39, 88.22, 117.31, 119.63, 125.38, 125.62, 129.55, 131.29, 141.83, 151.69, 152.27, 154.12, 156.02, 158.52. MS (API-ESI): *m/z* 396.77 $[M+H]^+$. Anal. calcd. For ($C_{16}H_{15}ClFN_5O_4$) C, 48.56; H, 3.82; N, 17.70; Found: C, 48.55; H, 3.83; N, 17.71.

2-Chloro-*N*^{6}-(4-chloro-2-fluorophenyl)amino-9*H*-(*β*-D-ribofuranosyl)adenine (26).

Reaction of **22** (250 mg, 0.558 mmol) with 4-chloro-2-fluoroaniline (130 mg, 99.1 μL, 0.892 mmol) for 10 h followed by deprotection gave **26**, which was purified by chromatography on a silica gel column ($CHCl_3$-MeOH, 99:1) as a white solid (156 mg, 65% yield).^{1}H NMR (DMSO-d_6): δ 3.51-3.72 (2m, 2H, H-5′), 3.94 (d, *J* = 3.63 Hz, 1H, H-4′), 4.05-4.15 (m, 1H, H-3′), 4.52 (q, *J* = 5.77 Hz, 1H, H-2′), 5.31 (t, *J* = 5.55 Hz, 1H, OH), 5.21 (d, *J* = 5.13 Hz, 1H, OH), 5.51 (d, *J* = 5.98 Hz, 1H, OH), 5.86 (d, *J* = 5.99 Hz, 1H, H-1′), 7.32 (d, *J* = 8.55 Hz, 1H, arom.), 7.52 (t, *J* = 4.28 Hz, 1H, arom.), 7.55 (d, *J* = 2.13 Hz, 1H, arom.), 8.53 (s, 1H, H-8), 10.21 (brs, 1H, NH). ^{13}C NMR (DMSO-d_6):61.92, 70.98, 74.45, 86.41, 88.15, 117.43, 119.69, 125.41, 125.57, 129.68, 131.32, 141.91, 151.73, 153.27, 154.01, 156.08, 158.58. MS (API-ESI): *m/z* 431.25 $[M+H]^+$. Anal. calcd. for ($C_{16}H_{14}Cl_2FN_5O_4$) C, 44.67; H, 3.28; N, 16.28; Found: C, 44.68; H, 3.27; N, 16.29.

General procedure for the Synthesis of 2′,3′-*O*-Isopropylidene derivatives 29, and 30.

A mixture of **25** or **26** (1 equiv), 2,2-dimethoxypropane (18.1 equiv) and camphorsulfonic acid (1 equiv) in anhydrous acetone (10 mL) was stirred at 55 °C for the time reported below. The solvent

was removed in vacuo, and the residue was purified by column chromatography to afford the desired compounds.

N^6-(4-Chloro-2-fluorophenyl)amino-9*H*-(2,3-*O*-isopropylidene-*β*-D-ribofuranosyl)adenine (29).

The title compound was synthesized from **25** (200 mg, 0.505 mmol, reaction time 6 h). Chromatography on a silica gel column ($CHCl_3$-MeOH, 98:2) gave **29** as a white foam (209 mg, 95% yield). ^{1}HNMR (DMSO-d_6): δ 1.36 (s, 3H, CH_3), 1.52 (s, 3H, CH_3), 3.41-3.62 (m, 2H, H-5′), 4.24 (dt, J = 2.70, 5.10 Hz, 1H, H-4′), 4.95 (dd, J = 2.40 Hz, 1H, H-3′), 5.25 (t, J = 5.60 Hz, 1H, OH), 5.36 (dd, J = 3.22, 6.30 Hz, 1H, H-2′), 6.16 (d, J = 2.4 Hz, 1H, H-1′), 7.3 (dd, J = 4.50, 9.20 Hz, 1H, arom.), 7.5 (dd, J = 6.50, 10.40 Hz, 1H, arom.), 7.61 (t, J = 8.40 Hz, 1H, arom.), 8.29 (s, 1H, H-2), 8.52 (s, 1H, H-8), 9.71 (s, 1H, NH). MS (API-ESI): *m/z* 436.837 $[M+H]^+$. Anal. calcd. for ($C_{19}H_{19}ClFN_5O_4$) C, 52.36; H, 4.39; N, 16.07; Found: C, 52.37; H, 4.38; N, 16.06.

2-Chloro-N^6-(4-chloro-2-fluorophenyl)amino-9*H*-(2,3-*O*-isopropylidene-*β*-D-ribofuranosyl)-adenine (30).

The title compound was obtained starting from **26** (150 mg, 0.348 mmol, reaction time 2 h). Chromatography on a silica gel column ($CHCl_3$-MeOH, 97:3) gave **30** as a white foam (136 mg, 83% yield). ^{1}H NMR (DMSO-d_6): δ 1.32 (s, 3H, CH_3), 1.51 (s, 3H, CH_3), 3.51 (m, 2H, H-5′), 4.22 (pd, J = 3.0 Hz, 1H, H-4′), 4.93 (dd, J =1.93, 6.20 Hz, 1H, H-3′), 5.06 (t, J = 5.13 Hz, 1H, OH), 5.3 (dd, J = 2.56, 5.98 Hz, 1H, H-2′), 6.11 (d, J = 2.13 Hz, 1H, H-1′), 7.31 (dd, J = 1.71, 8.12 Hz, 1H, arom.), 7.48-7.56 (m, 2H, arom.), 8.47 (s, 1H, H-8), 10.22 (s, 1H, NH). MS (API-ESI): *m/z* 471.28 $[M+H]^+$. Anal. calcd. For ($C_{19}H_{18}Cl_2FN_5O_3$) C, 48.53; H, 3.86; N, 14.89; Found: C, 48.54; H, 3.87; N, 14.87.

General procedure for the Synthesis of Compounds 31-34.

Compounds **27-30** (1 equiv) in dry acetonitrile (10 mL) under nitrogen atmosphere were stirred with cooling to -5 °C. $SOCl_2$ (3 equiv) was added portionwise followed by dry pyridine (2 equiv) and allowed to react for 30 min at -5° C, then allowed to warm to room temperature and stirred for 6 h. The procedure was repeated after 6 h, and the mixture was stirred at room temperature overnight. Water was added (5 mL), and the solution was neutralized with $NaHCO_3$ (1 M) and extracted with CH_2Cl_2 (3 × 10 mL). The organic layer was dried (Na_2SO_4), and the solvent was evaporated to dryness. The residue was purified by column chromatography as reported below.

N^6-(*R*)-3-Tetrahydrofuranyl-9*H*-(2,3-*O*-isopropylidene-5-chloro-5-deoxy-*β*-D-ribofuranosyl) adenine (31).

The title compound was synthesized from **27** (290 mg, 0.768 mmol). Chromatography on a silica gel column ($CHCl_3$-MeOH, 99:1) gave **31** as a white foam (167 mg, 55% yield). ^{1}H NMR (DMSO-d_6): δ 1.38 (s, 3H, CH_3), 1.55 (s, 3H, CH_3), 1.95-2.23 (2m, 2H, tetrahydrofuranyl), 3.60 (dd, J = 4.52, 8.80 Hz, 1H, tetrahydrofuranyl), 3.72 (q, J = 7.70 Hz, 1H, tetrahydrofuranyl), 3.80-3.96 (m, 4H, tetrahydrofuranyl, H-5′), 4.08 (q, J = 5.30 Hz, 1H, H-4′), 4.20 (q, J = 4.70 Hz, 1H, H-3′), 4.58-4.71 (m, 1H, NHC*H*), 4.74 (q, J = 5.30 Hz, 1H, H-2′), 5.92 (d, J = 5.50 Hz, 1H, H-1′), 7.98 (brs, 1H, NH), 8.22 (brs, 1H, H-2), 8.38 (s, 1H, H-8). MS (API-ESI): *m/z* 396.8 $[M+H]^+$. Anal. calcd. for ($C_{17}H_{22}ClN_5O_4$) C, 51.58; H, 5.60; N, 17.69; Found: C, 51.57; H, 5.61; N, 17.68.

2-Chloro-N^6-(*R*)-3-tetrahydrofuranyl-9*H*-(2,3-*O*-isopropylidene-5-chloro-5-deoxy-*β*-D-ribofuranosyl)adenine (32).

The title compound was synthesized from **28** (300 mg, 0.728 mmol). Chromatography on a silica gel column ($CHCl_3$-MeOH, 99:1) gave **32** as a white foam (204 mg, 65% yield). ^{1}H NMR (DMSO-d_6): δ 1.35 (s, 3H, CH_3), 1.52 (s, 3H, CH_3), 1.85-2.28 (m, 2H, tetrahydrofuranyl), 3.55-3.81 (m, 4H, tetrahydrofuranyl), 3.81-3.92 (m, 2H, H-5′), 4.3-4.36 (m, 1H, H-4′), 4.62 (brs, 1H,

NH*CH*), 5.1 (q, *J* = 3.02 Hz, 1H, H-3′), 5.37 (dd, *J* = 2.99, 6.20 Hz, 1H, H-2′), 6.19 (s, 1H, H-1′), 8.38 (s, 1H, H-8), 8.62 (brs, 1H, NH). MS (API-ESI): *m/z* 431.28 $[M+H]^+$. Anal. calcd. for ($C_{17}H_{21}N_5O_4Cl_2$) C, 47.45; H, 4.92; N, 16.28; Found: C, 47.46; H, 4.93; N, 16.27.

N^6-(4-Chloro-2-fluorophenyl)amino-9*H*-(2,3-*O*-isopropylidene-5-chloro-5-deoxy-*β*-D-ribofuranosyl)adenine (33).

The title compound was synthesized from **29** (300 mg, 0.688 mmol). Chromatography on a silica gel column ($CHCl_3$) gave **33** as a white foam (134 mg, 43% yield). ^{1}HNMR (DMSO-d_6): δ 1.32 (s, 3H, CH_3), 1.52 (s, 3H, CH_3), 3.75 (dd, *J* = 6.42, 11.12 Hz, 1H, H-5′) 3.85 (dd, *J* = 6.84, 11.12 Hz, 1H, H-5′), 4.36 (dt, *J* = 2.99, 6.41 Hz, 1H, H-4′), 5.08 (dd, *J* = 2.99, 6.41 Hz, 1H, H-3′), 5.51 (dd, *J*= 2.35, 6.21 Hz, 1H, H-2′), 6.23 (d, *J* = 2.56 Hz, 1H, H-1′), 7.29 (dd, *J* = 1.28, 8.55 Hz, 1H, arom.), 7.52 (dd, *J* = 2.14, 10.26 Hz, 1H, arom.), 7.61 (t, *J* = 8.55 Hz, 1H, arom.), 8.33 (s, 1H, H-2), 8.48 (s, 1H, H-8), 9.76 (s, 1H, NH). MS (API-ESI): *m/z* 455.28 $[M+H]^+$. Anal. calcd. for ($C_{19}H_{18}Cl_2FN_5O_3$) C, 50.23; H, 3.99; N, 15.42; Found: C, 50.21; H, 3.97; N, 15.43.

2-Chloro-N^6-(4-chloro-2-fluorophenyl)amino-9*H*-(2,3-*O*-isopropylidene-5-chloro-5-deoxy-*β*-D-ribofuranosyl)adenine (34).

The title compound was synthesized from **30** (270 mg, 0.574 mmol). Chromatography on a silica gel column ($CHCl_3$) gave **34** as a white foam (216 mg, 77% yield). ^{1}HNMR (DMSO-d_6): δ 1.38 (s, 3H, CH_3), 1.58 (s, 3H, CH_3), 3.77 (dd, *J* = 6.19, 11.32 Hz, 1H, H-5′), 3.86 (dd, *J* = 6.83, 11,12 Hz, 1H, H-5′), 4.35 (dt, *J* = 3.02, 6.41 Hz, 1H, H-4′), 5.03 (dd, *J* = 2.99, 5.99 Hz, 1H, H-3′), 5.41 (dd, *J* = 2.14, 5.98 Hz, 1H, H-2′), 6.21 (d, *J* = 1.71 Hz, 1H, H-1′), 7.31 (dd, *J* = 2.14, 8.55 Hz, 1H, arom.), 7.53 (m, 2H, arom.), 8.48 (s, 1H, H-8), 10.22 (s, 1H, NH). MS (API-ESI): *m/z* 489.73 $[M+H]^+$. Anal. calcd. for ($C_{19}H_{17}Cl_3FN_5O_3$) C, 46.69; H, 3.51; N, 14.33; Found: C, 46.67; H, 3.53; N, 14.35.

Membrane preparation. Membranes for radioligand binding were prepared as described previously.[35] In brief, after homogenization of CHO cells stably transfected with the hAR subtype membranes were prepared in a two-step procedure. A first low-speed centrifugation (1,000 x g) was used to remove cell fragments and nuclei and was followed by a high-speed centrifugation (100,000 x g) of the supernatant in order to sediment a crude membrane fraction. The resulting membrane pellets were resuspended in the buffer used for the respective binding experiments, frozen in liquid nitrogen and stored in aliquots at -80°C. Adenylyl cyclase activity was measured in a membrane fraction obtained in a simplified procedure with only one high-speed centrifugation of the homogenate. The resulting crude membrane pellet was resuspended in 50 mM Tris/HCl, pH 7.4 and used immediately for the cyclase assay.

Radioligand binding and Adenylyl Cyclase Assay. In competition experiments the following radioligands were used: 1 nM [^{3}H]CCPA for hA_1ARs, 10 nM [^{3}H]NECA for hA_{2A}ARs, 1 nM [^{3}H]HEMADO for hA_3ARs.[35,38] Nonspecific binding of [^{3}H]CCPA was determined in the presence of 1 mM theophylline, while nonspecific binding of [^{3}H]NECA and [^{3}H]HEMADO was estimated in the presence of 100 µM (R)-*N*^{6}phenylisopropyladenosine (R-PIA). Dissociation constants (K_i-values) were calculated from radioligand competition experiments utilizing the program Prism (GraphPad, San Diego, CA, USA).

Due to the lack of a useful high-affinity radioligand for A_{2B} adenosine receptors, stimulation of adenylyl cyclase activity was measured to determine agonist potency (EC_{50} values).[35] If only partial agonistic activity was observed, efficacy was compared to 100 µM NECA as a full agonist. All values are given as geometric means with 95% confidence intervals ($n \geq 3$). The functional activity at the hA_1, A_{2A}, and A_3 receptors was determined in adenylyl cyclase experiments. The inhibition of forskolin-stimulated adenylyl cyclase via hA_1 and A_3 receptors was measured as described earlier.[49] As reference agonists (efficacy = 100%), CCPA and NECA, respectively, were

used. Compounds were considered to be A_3 antagonists if they fully reversed (>85%) the NECA-mediated inhibition of adenylyl cyclase activity (IC_{50} values in Table 3).

Computational Chemistry. Molecular modeling and graphics manipulations were performed using MOE (Molecular Operating Environment, version 2013.08, Chemical Computing Group, Toronto, Canada) and UCSF-CHIMERA 1.8.1 (http://www.cgl.ucsf.edu/chimera) software packages, running on an E4 Computer Engineering E1080 workstation provided with an Intel Xeon processor. GOLD Suite 5.4.1 docking package (CCDC Software Limited: Cambridge, U.K., 2008)[39] was used for all docking calculations. Figures were generated using Pymol 1.8.2 (Schrödinger, LLC, New York, NY, 2016).

Residue Indexing. The Ballesteros−Weinstein double-numbering system[46] was used to describe the transmembrane (TM) location of the amino acids. Along with numbering their positions in the primary amino acid sequence, the residues have numbers in parentheses (X.YZ) that indicate their position in each transmembrane (TM) helix (X), relative to a conserved reference residue in that TM helix (YZ).

Three-Dimensional Structure of hA_1AR. In this study we used a previously published hA_1AR homology model,[50] built by means of the homology modeling tools implemented in the MOE suite. In particular, the crystal structure of the $hA_{2A}AR$ cocrystallized with the agonist UK-432097 (PDB ID: 3QAK),[44] was selected as a template for the entire hA_1AR structure. The hA_1AR sequence was retrieved from the publicly available sequence database www.uniprot.org and aligned against the sequence of the respective $A_{2A}AR$ template, taking into account the highly conserved residues in each TM domain and following the numbering scheme by Ballesteros and Weinstein.[46] Then, a homology model was built using the automated Homology Modeling protocol implemented in the MOE suite.

Docking Simulations of 5′-pyrazolyl adenosine derivatives at the hA_1AR Model. Structures of compounds **6**, **12**, **14**, and **16** were built using the builder tool implemented in the MOE suite and subjected to a MMFF94x energy minimization until a rms gradient was <0.05 kcal mol^{-1} $Å^{-1}$. Molecular docking of the ligands at the hA_1AR model was performed by means of the GOLD software, which uses a genetic algorithm and considers full ligand conformational flexibility and partial protein flexibility, i.e. the flexibility of side chain residues only. The coordinates of four key residues in the binding pocket of hA_1AR model, that is F (EL2), $N^{6.55}$, $W^{6.48}$ and $H^{7.43}$, were chosen as active-site origin. The active-site radius was set equal to 13 Å. The mobility of $T^{3.36}$, $W^{6.48}$, $H^{6.52}$, $N^{6.55}$, $T^{7.42}$, and $H^{7.43}$ side chains was set up using the flexible sidechains option in the GOLD front end, which incorporates the Lovell rotamer library.[51] Each GA run used the default parameters of 100 000 genetic operations on an initial population of 100 members divided into five subpopulations, with weights for crossover, mutation, and migration being set to 95, 95, and 10, respectively. GOLD allows a user-definable number of GA runs per ligand, each of which starts from a different orientation. For these experiments, the number of GA runs was set to 200 without the option of early termination, and scoring of the docked poses was performed with the original ChemPLP scoring function followed by rescoring with ChemScore.[41] The final receptor–ligand complex for each ligand was chosen interactively by selecting the highest scoring pose that was consistent with experimentally-derived information about the binding mode of the ligand.

Formalin Test. Adult male BLC57/6 mice (25-30 g) were housed three per cage under controlled illumination (12 h light/12 h dark cycle; light on 06:00 h) and standard environmental conditions (room temperature 20-22 °C, humidity 55-60%) for at least 1 week before the beginning of the experiments. Chow and tap water were available ad libitum. All surgery and experimental procedures were performed during the light cycle and were approved by the Animal Ethics Committee of the University of Campania “L. Vanvitelli”. Animal care was in compliance with European regulations on the protection of laboratory animals (O.J. of E.C. L358/1 18/12/86). All

efforts were made to reduce both animal suffering and the number of animals used during the experiments, as required by the Ethical Guidelines of the IASP. Formalin-induced pain is a widely used test for persistent pain.[48] Thirty microlitres of formalin (1.25%) were injected subcutaneously into the dorsal surface of the hind paws of awake mice using a 30-gauge needle. Nociceptive responses were divided into two phases: an initial early short phase (0-7 min) caused by a primary afferent discharge produced by the stimulus and followed by a quiescent period, and a second prolonged phase (15-60 min) of tonic pain. Each mouse was placed in a plexiglas testing chamber to acclimatize for 30 min. A mirror was placed at a 45° angle under the cage to allow a full view of the hind paws. Intraperitoneal vehicle (10% DMSO in 0.9% NaCl) or different doses of compounds **5**, **6**, **12** or **50** were administered 10 min before formalin in groups of 8-10 animals per treatment. Immediately following formalin injection, mice were observed for 60 min by experimenters who were blinded to the treatment. Pain-related behaviour was assessed using the following criteria: (1) paw lifting and the injected paw was lifted off the cage floor; (2) paw licking and the injected paw was licked or bitten. The time spent lifting or licking the injected paw was recorded every 5 min and expressed in minutes as mean ± SEM.

ASSOCIATED CONTENT

Supporting Information

The Supporting Information is available free of charge on the ACS Publications website at DOI:

Representative binding curves at hA_1AR, $hA_{2A}AR$ and hA_3AR for compounds **6**, **7**, **10**, **12**, **16** and **17**. Representative functional assays at hA_1AR, and hA_3AR for compounds **6**, **7**, **10**, **12**, **16** and **17**. Representative functional assays at $hA_{2B}AR$ for compounds **6** and **7**. Molecular formula strings (CSV).

AUTHOR INFORMATION

Corresponding Author

*(L.C.) email: loredana.cappellacci@unicam.it Tel: +39-0737-402228; fax +39-0737-637345; (A.L.) email: antonio.lavecchia@unina.it Tel: +39-081-678613/623; fax +39-081-678012

Notes

The authors declare no competing financial interest. #This work was presented in part at the 6th Joint German-Italian Purine Club Meeting, Purines 2015, Hamburg, Germany, July 2015.

Funding Sources

This work was financially supported by Fondo di Ricerca di Ateneo, University of Camerino (Grant FAR 2011/12 STI000044 to L.C. and Grant FAR 2014/15 FPI000044 to R.P.), by the Italian MIUR funds (Grant 20094BJ9R7 to L.C., and Grant 200928EEX4_004 to R.P.).

ACKNOWLEDGMENTS

We express our gratitude to Prof. Mario Grifantini and Prof. Palmarisa Franchetti for their suggestions and comments for this manuscript.

ABBREVIATIONS USED

A_1AR, A_1 adenosine receptor; A_{2A}AR, A_{2A} adenosine receptor; A_{2B}AR, A_{2B} adenosine receptor; A_3AR, A_3 adenosine receptor; CHO, Chinese hamster ovary; CCPA, 2-chloro-N^6-cyclopentyladenosine; CPA, N^6-cyclopentyladenosine; 5′-Cl-CPA, 5′-chloro-5′-deoxy-N^6-cyclopentyladenosine; 5′-Cl-CCPA, 2,5′-dichloro-5′-deoxy-N^6-cyclopentyladenosine; 5′Cl5′d-(±)-ENBA, 5′-chloro-5′-deoxy-N^6-(±)-*endo*-(norborn-2-yl)adenosine; 3,5-DMP, 3,5-dimethyl-pyrazolyl; DPCPX, 8-cyclopentyl-1,3-dipropylxanthine; (±)-ENBA, N^6-(±)-*endo*-(norborn-2-yl)adenosine; GPCR, G-protein-coupled receptor; HEMADO, 2-(hexyn-1-yl)-N^6-methyladenosine; i.p., intraperitoneal; NECA, 5'-*N*-ethylcarboxamidoadenosine; R-PIA, (*R*)-N^6-phenylisopropyladenosine; Et_3N, Triethylamine; TM, transmembrane helical domain.

REFERENCES

(1) Fredholm, B. B.; IJzerman, A. P.; Jacobson, K. A.; Linden, J.; Muller, C. Nomenclature and classification of adenosine receptors an update. *Pharmacol. Rev.* **2011**, *63*, 1−34.

(2) Jacobson, K. A.; Muller, C. E. Medicinal chemistry of adenosine, P2Y and P2X receptors. *Neuropharmacology* **2016**, *104*, 31-49.

(3) Donegan, R. K.; Lieberman, R. L. Discovery of molecular therapeutics for glaucoma: challenges, successes, and promising directions miniperspective. *J. Med. Chem.* **2016**, *59*, 788-809.

(4) Luongo, L.; Malcangio, M.; Salvemini, D.; Starowicz, K. Chronic pain: new insights in molecular and cellular mechanisms. *Biomed. Res. Int.* **2015**, *2015*, 676725.

(5) Sawynok, J. Adenosine receptor targets for pain. *Neuroscience* **2016**, *338*, 1-18.

(6) Janes, K.; Symons-Liguori, A. M.; Jacobson, K. A.; Salvemini, D. Identification of A_3 adenosine receptor agonists as novel non-narcotic analgesics. *Br. J. Pharmacol.* **2016**, *173*, 1253–1267.

(7) Jacobson, K. A.; Gao, Z. G. Adenosine receptors as therapeutic targets. *Nat Rev Drug Discov.* **2006**, *5*, 247-264.

(8) Knutsen, L. J.; Petersen, H.; Thomsen, C.; Weis, J. U.; Shalmi, M.; Judge, M.E.; Hansen, A. J.; Sheardown, M. J. N-substituted adenosines as novel neuroprotective A1 agonists with diminished hypotensive effects. *J. Med. Chem.* **1999**, *42*, 3463-3477.

(9) Elzein, E.; Zablocki, J. A_1 adenosine receptor agonists and their potential therapeutic applications. *Expert Opin Investig Drugs* **2008**, *17*, 1901-1910.

(10) Gao, Z.-G.; Jacobson, K. A. Emerging adenosine receptor agonists – an update. *Expert Opin. Emerging Drugs* **2011**, *16*, 597-602.

(11) Franchetti, P.; Cappellacci, L.; Marchetti, S.; Trincavelli, L.; Martini, C.; Mazzoni, M.R.; Lucacchini, A.; Grifantini, M. 2′-*C*-Methyl analogues of selective adenosine receptor agonists: synthesis and binding studies. *J. Med. Chem.* **1998**, *41*, 1708-1715.

(12) Cappellacci, L.; Franchetti, P.; Pasqualini, M.; Petrelli, R.; Vita, P.; Lavecchia, A.; Novellino, E.; Costa, B.; Martini, C.; Klotz, K.N.; Grifantini M. Synthesis, biological evaluation, and molecular modeling of ribose-modified adenosine analogues as adenosine receptor agonists. *J. Med. Chem.* **2005**, *48*, 1550-1562.

(13) Cappellacci, L.; Franchetti, P.; Vita, P.; Petrelli, R.; Lavecchia, A.; Costa, B.; Spinetti, F.; Martini, C.; Klotz, K.N.; Grifantini, M. 5′-Carbamoyl derivatives of 2′-C-methylpurine nucleosides as selective A_1 adenosine receptor agonists: affinity, efficacy, and selectivity for A_1 receptor from different species. *Bioorg. Med. Chem.* **2008**, *16*, 336-353.

(14) Franchetti, P.; Cappellacci, L.; Vita, P.; Petrelli, R.; Lavecchia, A.; Kachler, S.; Klotz, K.-N.; Marabese, I.; Luongo, L.; Maione, S.; Grifantini, M. N^6-Cycloalkyl- and N^6- bicycloalkyl-C5′(C2′)-modified adenosine derivatives as high-affinity and selective agonists at the human A_1 adenosine receptor with antinociceptive effects in mice. *J. Med. Chem.* **2009**, *52*, 2393−2406.

(15) Maione, S.; de Novellis, V.; Cappellacci, L.; Palazzo, E.; Vita, D.; Luongo, L.; Stella, L.; Franchetti, P.; Marabese, I.; Rossi, F.; Grifantini, M. The antinociceptive effect of 2- chloro-2′-C-methyl-*N*6-cyclopentyladenosine (2′-Me-CCPA), a highly selective adenosine A_1 receptor agonist in the rat. *Pain* **2007**, *3*, 281-292.

(16) Petrelli, R.; Torquati, I.; Kachler, S.; Luongo, L.; Maione, S.; Franchetti, P., Grifantini, M., Novellino, E.; Lavecchia, A.; Klotz, K.-N.; Cappellacci, L. 5′-*C*-Ethyl-tetrazolyl-N^6-substituted adenosine and 2-chloroadenosine as highly potent dual acting A_1 adenosine receptor agonists and A_3 adenosine receptor antagonists. *J. Med. Chem.* **2015**, *58*, 2560-2566.

(17) Petrelli, R.; Grifantini, M.; Cappellacci, L. Development of C-methyl branched purine ribonucleoside analogs: chemistry, biological activity and therapeutic potential. *Curr. Med. Chem.* **2016**, *23*, 3118-3135.

(18) Palle, V. P.; Varkhedkar, V.; Ibrahim, P.; Ahmed, H.; Li, Z.; Gao, Z.; Ozeck, M.; Wu, Y.; Zeng, D.; Wu, L.; Leung, K.; Chuc, N.; Zablocki, J. A. Affinity and intrinsic efficacy (IE) of 5'-carbamoyl adenosine analogues for the A_1 adenosine receptor-efforts towards the discovery of a

chronic ventricular rate control agent for the treatment of atrial fibrillation (AF). *Bioorg. Med. Chem. Lett.* **2004**, *14*, 535–539.

(19) Carlin, J. L.; Jain, S.; Gizewski, E.; Wan, T. C.; Tosh, D. K.; Xiao, C.; Auchampach, J. A.; Jacobson, K. A.; Gavrilova, O.; Reitman, M. L. Hypothermia in mouse is caused by adenosine A1 and A_3 receptor agonists and AMP via three distint mechanisms. *Neuropharmacology* **2017**, *114*, 101-113.

(20) Luongo, L.; Petrelli, R.; Gatta, L.; Giordano, C.; Guida, F.; Vita, P.; Franchetti, P.; Grifantini, M.; de Novellis, V.; Cappellacci, L.; Maione, S. 5′-Chloro-5′-deoxy-(±)-ENBA, a potent and selective adenosine A_1 receptor agonist, alleviates neuropathic pain in mice through functional glial and microglial changes without affecting motor or cardiovascular functions. *Molecule*s **2012**, *17*, 13712-13726.

(21) Luongo, L.; Guida, F.; Imperatore, R.; Napolitano, F.; Gatta, L.; Cristino, L.; Giordano, C.; Siniscalco, D.; Di Marzo, V.; Bellini, G.; Petrelli, R.; Cappellacci, L.; Usiello, A.; de Novellis, V.; Rossi, F.; Maione, S. The A1 Adenosine receptor as a new player in microglia physiology. *Glia* **2014**, *62*, 122-132.

(22) Mango, D.; Bonito-Oliva, A.; Ledonne, A.; Cappellacci, L.; Petrelli, R.; Nisticò, R.; Berretta, N.; Fisone, G.; Mercuri, N. B. Adenosine A_1 receptor stimulation reduces D1 receptor-mediated GABAergic transmission from striatonigral terminals and l-DOPA-induced dyskinesia in dopamine denervated mice. *Exp. Neurol.* **2014**, *261*, 733-743.

(23) Fishman, P.; Bar-Yehuda, S.; Liang, B. T.; Jacobson, K. A. Pharmacological and therapeutic effects of A_3 adenosine receptor agonists. *Drug Discov Today* **2012**, *17*, 359-366.

(24) Fishman, P.; Cohen, S. The A_3 adenosine receptor (A_3AR): therapeutic target and predictive biological marker in rheumatoid arthritis. *Clin. Rheumatol.* **2016**, *35*, 2359-2362.

(25) Chen, Z.; Janes, K.; Chen, C.; Doyle, T.; Bryant, L.; Tosh, D. K., Jacobson, K. A.; Salvemini, D. Controlling murine and rat chronic pain through A_3 adenosine receptor activation. *FASEB J.* **2012**, *26*, 1855–1865.

(26) Little, J. W.; Ford, A.; Symons-Liguori, A. M.; Chen, Z.; Janes, K.; Doyle, T., Xie, J.; Luongo, L.; Tosh, D. K.; Maione, S.; Bannister, K.; Dickenson, A. H.; Vanderah, T. W.; Porreca, F.; Jacobson K. A.; Salvemini, D. Endogenous adenosine A_3 receptor activation selectively alleviates persistent pain states. *Brain* **2015**, *138*, 28–35.

(27) Jacobson, K. A. and Civan, M. M. Ocular purine receptors as drug targets in the eye. *J. Ocul. Pharmacol. Ther*. **2016**, *32*, 534-547.

(28) Hua, X.; Chason, K. D.; Fredholm, B. B.; Deshpande, D. A.; Penn, R. B.; Tilley, S. L. Adenosine induces airway hyperresponsiveness through activation of A_3 receptors on mast cells. *J. Allergy Clin. Immunol.* **2008**, *122*, 107-113.

(29) Bulger, E. M.; Tower, C. M.; Warner, K. J.; Garland, T.; Cuschieri, J.; Rizoli, S.; Rhind, S.; Junger, W. G. Increased neutrophil adenosine A_3 receptor expression is associated with hemorrhagic shock and injury severity in trauma patients. *Shock* **2011**, *36*, 435-439.

(30) Petrelli, R.; Scortichini, M.; Kachler, S.; Luongo, L.; Torquati, I.; Del Bello, F.; Novellino, E.; Maione, S.; Lavecchia, A.; Klotz, K.-N.; Cappellacci, L. Exploring the role of N^6-substituents in potent dual acting 5'-C-ethyl-tetrazolyl-adenosine derivatives: synthesis, binding, functional assays and antinociceptive effects in mice. *J. Med. Chem.* **2017**, *60*, 4327-4341.

(31) Cappellacci, L.; Petrelli, R.; Franchetti, P.; Vita, P.; Kusumanchi, P.; Kumar, M.; Jayaram, H. N.; Zhou, B.; Yen, Y.; Grifantini, M. Synthesis and biological activity of novel N^6-substituted and 2,N^6-disubstituted adenine ribo- and 3′-*C*-methyl-ribonucleosides as antitumor agents. *Eur. J. Med. Chem.* **2011**, *46*, 1499-1504.

(32) Hou, X.; Lee, H. W.; Tosh, D. K.; Zhao, L. X.; Jeong, L. S. Alternative and improved syntheses of highly potent and selective A_3 adenosine receptor agonists, Cl-IB-MECA and thio-Cl-IB-MECA. *Arch. Pharm. Res.* **2007**, *30*, 1205–1209.

(33) Lum, R. T.; Pfister, J. R.; Schow, S. R.; Wick, M. M.; Nelson, M. G.; Schreiner, G. F. N^6 Heterocyclic Substituted Adenosine Derivatives. PCT Int. Appl. WO 98/08855, 1998.

(34) Zablocki, J. A.; Palle, V. P.; Ibrahim, P. N.; Varkhedkar,V.; Belardinelli, L. N^6 Heterocyclic 5' Modified Adenosine Derivatives. PCT Int. Appl. WO0140244 (A1), 2001.

(35) Klotz, K.-N.; Hessling, J.; Hegler, J.; Owman, B.; Kull, B.; Fredholm, B. B.; Lohse, M. J. Comparative pharmacology of human adenosine receptor subtypes-characterization of stably transfected receptors in CHO cells. *Naunyn-Schmiedeberg's Arch. Pharmacol*. **1998**, *357*, 1−9.

(36) Lohse, M. J.; Klotz, K.-N.; Schwabe, U.; Cristalli, G.; Vittori, S.; Grifantini, M. 2-Chloro-N^6-cyclopentyladenosine: a highly selective agonist at A_1 adenosine receptors. *Naunyn-Schmiedeberg's Arch. Pharmacol.* **1988**, *337*, 687-689.

(37) Prasad, R. N.; Bariana, D. S.; Fung, A.; Savic, M.; Tietje, K.; Stein, H. H.; Brondyk, H. D.; Egan, R. S. Modification of the 5′- position of purine nucleosides. 2. Synthesis and some cardiovascular properties of adenosine-5′-(N-substituted)carboxamides. *J. Med. Chem.* **1980**, *23*, 313-319.

(38) Klotz, K.-N.; Kachler, S.; Falgner, N.; Volpini, R.; Dal Ben, D.; Lambertucci, C.; Mishra, R. C.; Vittori, S.; Cristalli, G. [^{3}H]-HEMADO a novel highly potent and selective radiolabeled agonist for A_3 adenosine receptors. *Eur. J. Pharmacol.* **2007**, *556*, 14-18.

(39) Jones, G.; Willett, P.; Glen, R. C.; Leach, A. R.; Taylor, R. Development and validation of a genetic algorithm for flexible docking. *J. Mol. Biol.* **1997**, *267*, 727-748.

(40) Verdonk, M. L.; Giangreco, I.; Hall, R. J.; Korb, O.; Mortenson, N.; Murray, W. Docking performance of fragments and drug like compounds. *J. Med. Chem.* **2011**, *54*, 5422-5431.

(41) Verdonk, M. L.; Cole, J. C.; Hartshorn, M. J.; Murray, C. W.; Taylor, R. D. Improved protein-ligand docking using GOLD. *Proteins: Struct., Funct., Genet.* **2003**, *52*, 609-623.

(42) Glukhova, A.; Thal, D.T.; Nguyen, A.T.N.; Vecchio, E.A.; Jörg, M.; Scammells, P.J.; May, L.T.; Sexton, P.M.; Christopoulos A. Structure of the adenosine A_1 receptor reveals the basis for subtype selectivity. *Cell* **2017**, *168*, 867-877.

(43) Cheng, R.K.Y; Segala, E.; Robertson, N.; Deflorian, F.; Dorè, A.S.; Errey, J.C.; Fiez-Vandal, C.; Marshall, F.H.; Cooke, R.M. Structures of human A_1 and A_{2A} adenosine receptors with xanthines reveal determinants of selectivity. *Structure* **2017**, *25*, 1275-1285.

(44) Xu, F.; Wu, H.; Katritch, V.; Han, G. W.; Jacobson, K. A.; Gao, Z. G.; Cherezov, V.; Stevens, R. Agonist bound structure of the human adenosine A_{2A} receptor. *Science* **2011**, *332*, 322-327.

(45) Paoletta, S.; Tosh, D. K.; Finley, A.; Gizewski, E.; Moss, S. M.; Gao, Z. G.; Auchampach, J. A.; Salvemini, D.; Jacobson, K. A. Rational design of sulfonated A_3 adenosine receptor-selective nucleosides as pharmacological tools to study chronic neuropathic pain. *J. Med. Chem.* **2013**, *56*, 5949-5963.

(46) Ballesteros, J. A.; Weinstein, H. Integrated methods for the construction of three dimensional models and computational probing of structure-function relationships in G-protein coupled receptors. *Methods Neurosci.* **1995**, *25*, 366-428.

(47) Lebon, G.; Warne, T.; Edwards, P. C.; Bennett, K.; Langmead, C. J.; Leslie, A. G. W.; Tate, C. G. Agonist-bound adenosine A_{2A} receptor structures reveal common features of GPCR activation. *Nature* **2011**, *474*, 521-525.

(48) Dubuisson, D.; Dennis, S. G. The formalin test: a quantitative study of the analgesic effects of morphine, meperidine, and brain stem stimulation in rats and cats. *Pain* **1977**, *4*, 161–174.

(49) Klotz, K. N.; Cristalli, G.; Grifantini, M.; Vittori, S.; Lohse, M. J.; Photoaffinity labeling of A_1-adenosine receptors. *J. Biol. Chem.* **1985**, *260*, 14659-14664.

(50) Tosh, D. K.; Phan, K.; Deflorian, F.; Wei, Q.; Gao, Z.; Jacobson, K. A. Truncated (*N*)-methanocarba nucleosides as A_1 adenosine receptor agonists and partial agonists: overcoming lack of a recognition element. *ACS Med. Chem. Lett.* **2011**, *2*, 626-631.

(51) Lovell, S. C.; Word, J. M.; Richardson, J. S.; Richardson, D. C. The penultimate rotamer library. *Proteins* **2000**, *40*, 389-408.

Scheme 1[a]

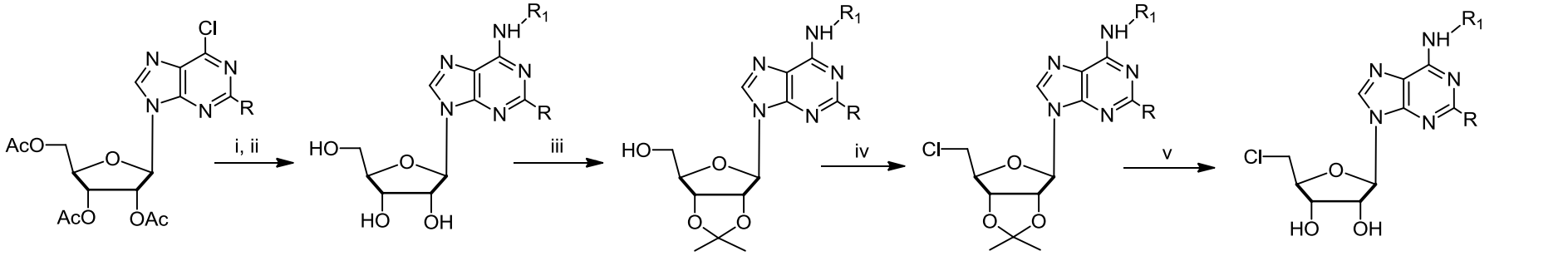

21. R = H
22. R = Cl

23. R = H, R_1 = (*R*)-3-tetrahydrofuranyl
24. R = Cl, R_1 = (*R*)-3-tetrahydrofuranyl
25. R = H, R_1 = 2F-4Cl-phenyl
26. R = Cl, R_1 = 2F-4Cl-phenyl

27. R = H, R_1 = (*R*)-3-tetrahydrofuranyl
28. R = Cl, R_1 = (*R*)-3-tetrahydrofuranyl
29. R = H, R_1 = 2F-4Cl-phenyl
30. R = Cl, R_1 = 2F-4Cl-phenyl

31. R = H, R_1 = (*R*)-3-tetrahydrofuranyl
32. R = Cl, R_1 = (*R*)-3-tetrahydrofuranyl
33. R = H, R_1 = 2F-4Cl-phenyl
34. R = Cl, R_1 = 2F-4Cl-phenyl

5. R = H, R_1 = (*R*)-3-tetrahydrofuranyl
6. R = Cl, R_1 = (*R*)-3-tetrahydrofuranyl
7. R = H, R_1 = 2F-4Cl-phenyl
8. R = Cl, R_1 = 2F-4Cl-phenyl

[a]Reagents and conditions : (i) R_1NH_2, EtOH, Et_3N, Δ; (ii) NH_3/MeOH, room temperature; (iii) 2,2-dimethoxypropane, camphorsulfonic acid, acetone, Δ; iv) $SOCl_2$, pyridine, CH_3CN, -5 °C to room temperature; (v) 70% HCOOH, 40 °C.

Scheme 2

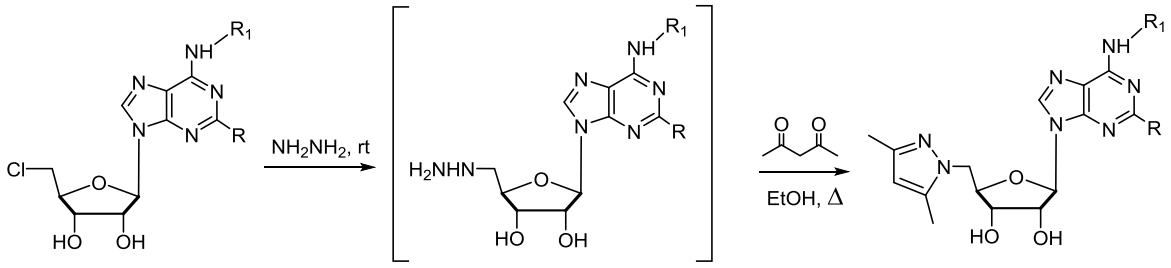

1. R = H, R_1 = cyclopentyl
2. R = Cl, R_1 = cyclopentyl
3. R = H, R_1 = *endo*-2-norbornyl
4. R = Cl, R_1 = *endo*-2-norbornyl
5. R = H, R_1 = (*R*)-3-tetrahydrofuranyl
6. R = Cl, R_1 = (*R*)-3-tetrahydrofuranyl
7. R = H, R_1 = 2F-4Cl-phenyl
8. R = Cl, R_1 = 2F-4Cl-phenyl

35 R = H, R_1 = cyclopentyl
36. R = Cl, R_1 = cyclopentyl
37. R = $NHNH_2$, R_1 = cyclopentyl
38. R = H, R_1 = *endo*-2-norbornyl
39. R = Cl, R_1 = *endo*-2-norbornyl
40. R = $NHNH_2$, R_1 = *endo*-2-norbornyl
41. R = H, R_1 = (*R*)-3-tetrahydrofuranyl
42. R = Cl, R_1 = (*R*)-3-tetrahydrofuranyl
43. R = $NHNH_2$, R_1 = (*R*)-3-tetrahydrofuranyl
44. R = H, R_1 = 2F-4Cl-phenyl
45. R = Cl, R_1 = 2F-4Cl-phenyl
46. R = $NHNH_2$, R_1 = 2F-4Cl-phenyl

9. R = H, R_1 = cyclopentyl
10. R = Cl, R_1 = cyclopentyl
11. R = H, R_1 = *endo*-2-norbornyl
12. R = Cl, R_1 = *endo*-2-norbornyl
13. R = H, R_1 = (*R*)-3-tetrahydrofuranyl
14. R = Cl, R_1 = (*R*)-3-tetrahydrofuranyl
15. R = H, R_1 = 2F-4Cl-phenyl
16. R = Cl, R_1 = 2F-4Cl-phenyl
17. R = 3,5-DMP, R_1 = cyclopentyl
18. R = 3,5-DMP, R_1 = *endo*-2-norbornyl
19. R = 3,5-DMP, R_1 = (*R*)-3-tetrahydrofuranyl
20. R = 3,5-DMP, R_1 = 2F-4Cl-phenyl

Table 1. Binding affinity of compounds 1-20 at A_1, A_{2A}, A_{2B} and A_3 adenosine receptors

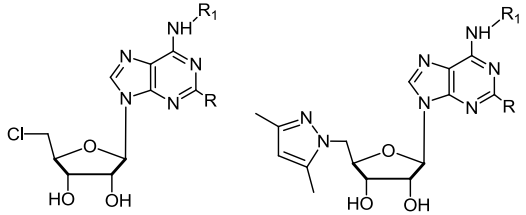

compd	R	R_1	K_i (nM)[a] A_1[b]	K_i (nM)[a] A_{2A}[c]	EC_{50} (nM)[a] A_{2B}[d]	K_i (nM)[a] A_3[e]
1	H	cyclopentyl	0.590 (0.460 – 0.761)	837 (585 – 1,200)	10,000 (7,580 – 13,200)	376 (285 – 496)
2	Cl	cyclopentyl	1.56 (1.31 – 1.87)	2,160 (1,560 – 2,980)	15,100 (9,930 – 22,900)	417 (339 – 513)
3	H	(±)-*endo*-2-norbornyl	0.510 (0.481 – 0.542)	1,340 (1,140 – 1,570)	8,530 (8,230 – 8,840)	1,290 (765 – 2,190)
4	Cl	(±)-*endo*-2-norbornyl	1.61 (0.950 – 2.74)	2,050 (1,380 – 3,030)	> 30,000	1,410 (968 – 2,070)
5	H	(*R*)-3-tetrahydrofuranyl	1.89 (1.60 – 2.24)	10,400 (9,970 – 10,800)	12,800 (11,900 – 13,800)	1,200 (908 – 1,600)
6	Cl	(*R*)-3-tetrahydrofuranyl	3.50 (3.07 – 3.98)	8,680 (6,740 – 11,200)	20,000 (14,200 – 28,200)	1,100 (992 – 1,230)
7	H	2-fluoro-4-chlorophenyl	1.87 (1.43 – 2.45)	1,360 (1,090 – 1,690)	3,740 (2,890 – 4,830)	136 (109 – 170)
8	Cl	2-fluoro-4-chlorophenyl	11.2 (8.58 – 14.5)	1,960 (1,780 – 2,160)	> 60,000	232 (207 – 261)
9	H	cyclopentyl	115 (104 – 128)	14,500 (11,100 – 18,900)	> 60,000	5,640 (3,400 – 9,330)
10	Cl	cyclopentyl	18.6 (14.7 – 23.5)	10,200 (6,870 – 15,200)	> 30,000	343 (277 – 425)
11	H	(±)-*endo*-2-norbornyl	25.6 (19.6 – 33.4)	19,600 (12,300 – 31,300)	> 30,000	5,450 (4,680 – 6,340)
12	Cl	(±)-*endo*-2-norbornyl	4.35 (3.63 – 5.22)	9,430 (6,770 – 13,100)	> 30,000	1,451 (1,150 – 1,830)
13	H	(*R*)-3-tetrahydrofuranyl	491 (461 – 522)	28,600 (23,900 – 34,200)	> 60,000	5,280 (4,330 – 6,450)
14	Cl	(*R*)-3-tetrahydrofuranyl	438 (330 – 582)	11,900 (9,450 – 15,000)	> 60,000	996 (724 – 1,371)
15	H	2-fluoro-4-chlorophenyl	158 (91.4 – 274)	6,830 (5,910 – 7,890)	> 60,000	2,730 (2,470 – 3,020)
16	Cl	2-fluoro-4-chlorophenyl	139 (123 – 157)	> 100,000	> 60,000	139 (109 – 177)
17	3,5-DMP	cyclopentyl	8.02 (5.36 – 12.0)	5,870 (5,100 – 6,750)	> 30,000	562 (494 – 639)
18	3,5-DMP	(±)-*endo*-2-norbornyl	59.4 (48.0 – 73.5)	10,500 (8,280 – 13,400)	> 60,000	667 (601 – 740)
19	3,5-DMP	(*R*)-3-tetrahydrofuranyl	24.6 (20.5 – 29.5)	5,090 (3,700 – 7,020)	> 60,000	1,000 (830 – 1220)
20	3,5-DMP	2-fluoro-4-chlorophenyl	91.4 (81.9 – 102)	4,320 (3,780 – 4,940)	> 60,000	636 (539 – 751)

[a] K_i and EC_{50} values are given in nM with 95% confidence intervals in parentheses. [b]Displacement of specific [^{3}H]2-chloro-N^6-cyclopentyladenosine (**47**, CCPA)[36] binding in CHO cells transfected with the recombinant hA_1AR. [c]Displacement of specific [^{3}H]adenosine-5'-*N*-ethyluronamide (**48**, NECA)[37] binding in CHO cells transfected with recombinant $hA_{2A}AR$. [d]EC_{50} values for stimulation of adenylyl cyclase activity. [e]Displacement of specific [^{3}H]2-(1-hexynyl)-N^6-methyladenosine (**49**, HEMADO)[38] binding in CHO cells transfected with recombinant hA_3AR. 3,5-DMP, 3,5-dimethyl-pyrazolyl. All points were measured in duplicates in at least 3 independent experiments.

Table 2. Selectivity ratios for binding affinities

			Selectivity	
compd	R	R_1	A_{2A}/A_1	A_3/A_1
1[a]	H	cyclopentyl	1419	637
2[a]	Cl	cyclopentyl	1385	267
3[a]	H	(±)-*endo*-2-norbornyl	2627	2530
4[a]	Cl	(±)-*endo*-2-norbornyl	1273	875
5	H	(*R*)-3-tetrahydrofuranyl	5503	635
6	Cl	(*R*)-3-tetrahydrofuranyl	2480	314
7	H	2-fluoro-4-chlorophenyl	727	73
8	Cl	2-fluoro-4-chlorophenyl	175	21
9	H	cyclopentyl	126	49
10	Cl	cyclopentyl	548	18
11	H	(±)-*endo*-2-norbornyl	765	213
12	Cl	(±)-*endo*-2-norbornyl	2168	333
13	H	(*R*)-3-tetrahydrofuranyl	58	11
14	Cl	(*R*)-3-tetrahydrofuranyl	27	2.3
15	H	2-fluoro-4-chlorophenyl	43	17
16	Cl	2-fluoro-4-chlorophenyl	>719	1
17	3,5-DMP	cyclopentyl	732	70
18	3,5-DMP	(±)-*endo*-2-norbornyl	177	11
19	3,5-DMP	(*R*)-3-tetrahydrofuranyl	207	41
20	3,5-DMP	2-fluoro-4-chlorophenyl	47	7

[a]Data from Franchetti *et al.*[14] 3,5-DMP, 3,5-dimethyl-pyrazolyl.

Table 3. Potencies of selected compounds at hA_1 and hA_3AR

			Adenylyl cyclase activity[a]	
compd	R	R_1	A_1 (EC_{50} nM)[b]	A_3 (IC_{50} nM)[c]
5	H	(*R*)-3-tetrahydrofuranyl	140 (113 - 175)	-
6	Cl	(*R*)-3-tetrahydrofuranyl	54.2 (50.7 – 57.9)	-
7	H	2-fluoro-4-chlorophenyl	56.0 (50.2 – 62.5)	4,140 (3,090 – 5,550)
10	Cl	cyclopentyl	541 (494 – 592)	1,910 (1,170 – 3,140)
12	Cl	(±)-*endo*-2-norbornyl	134 (110 – 163)	-
16	Cl	2-fluoro-4-chlorophenyl	5,570 (5,230 - 5,940)	701 (382 – 1,280)
17	3,5-DMP	cyclopentyl	577 (367 – 909)	1,940 (1,260 – 2,980)

[a] Adenylyl cyclase experiments: the compounds were tested in membranes from hA_1CHO and hA_3CHO cells. [b]All tested compounds are full agonists at the A_1AR (efficacy ≥90%, compared to CCPA as a full agonist). [c]All tested compounds reverted NECA-induced inhibition adenylyl cyclase activity and thus are antagonists at the hA_3AR. 3,5-DMP, 3,5-dimethyl-pyrazolyl. All points were measured in duplicates in at least 3 independent experiments.

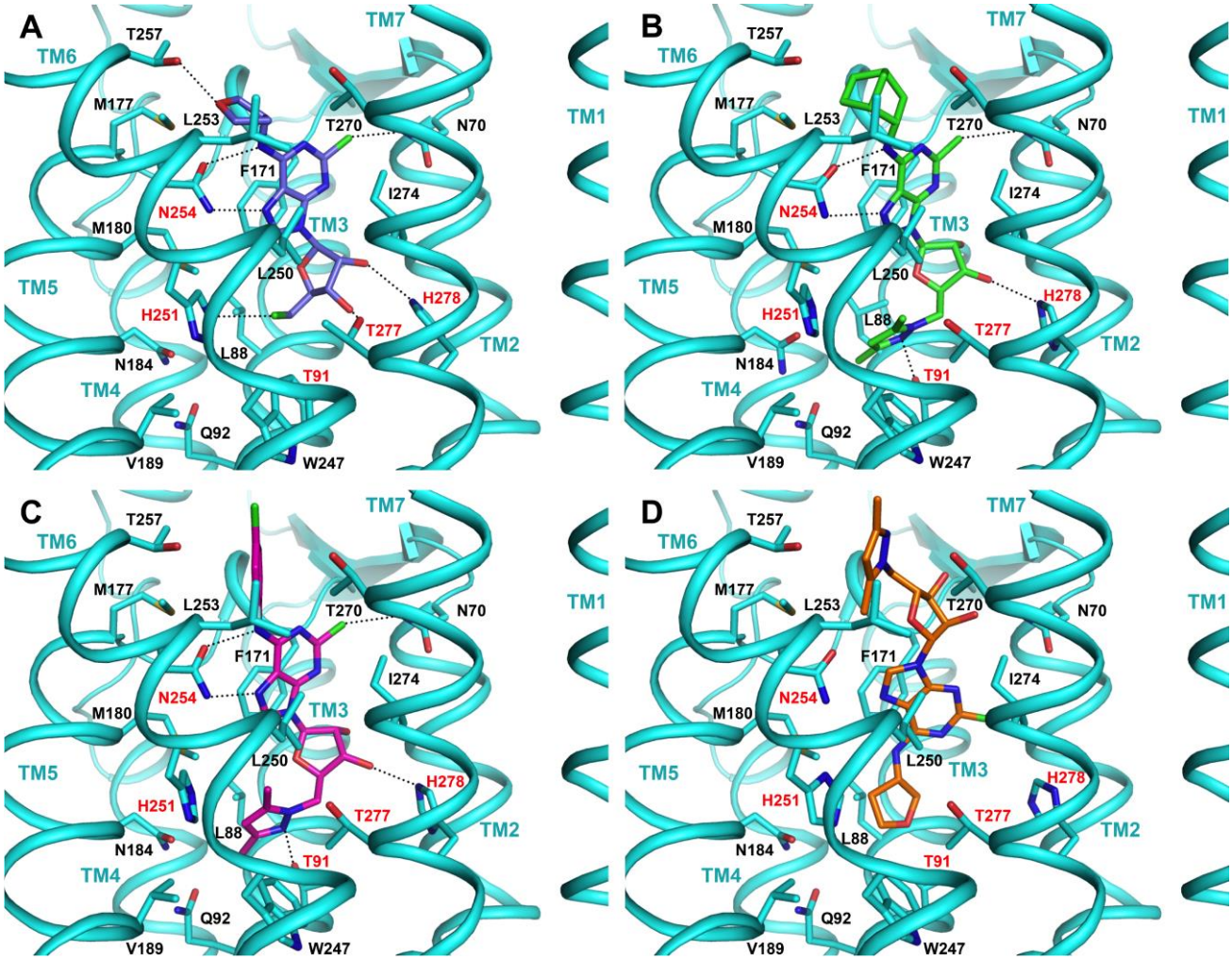

Figure 1. Putative binding modes of selected 5′-chloro adenosine derivative **6** (A, slate carbons), and 5′-pyrazolyl adenosine derivatives **12** (B, green carbons), **16** (C, magenta carbons), and **14** (D, orange carbons) obtained after docking simulations at the hA_1AR model (cyan ribbons). Poses are viewed from the membrane side. Ligands and interacting key residues (cyan carbon) are represented as stick models. The amino acids important for ligand recognition ($T91^{3.36}$, $H251^{6.52}$, $N254^{6.55}$, $T277^{7.42}$, $H278^{7.43}$) are labeled in red. H-bonding interactions are pictured as dotted black lines and non-polar hydrogens are undisplayed for clarity.

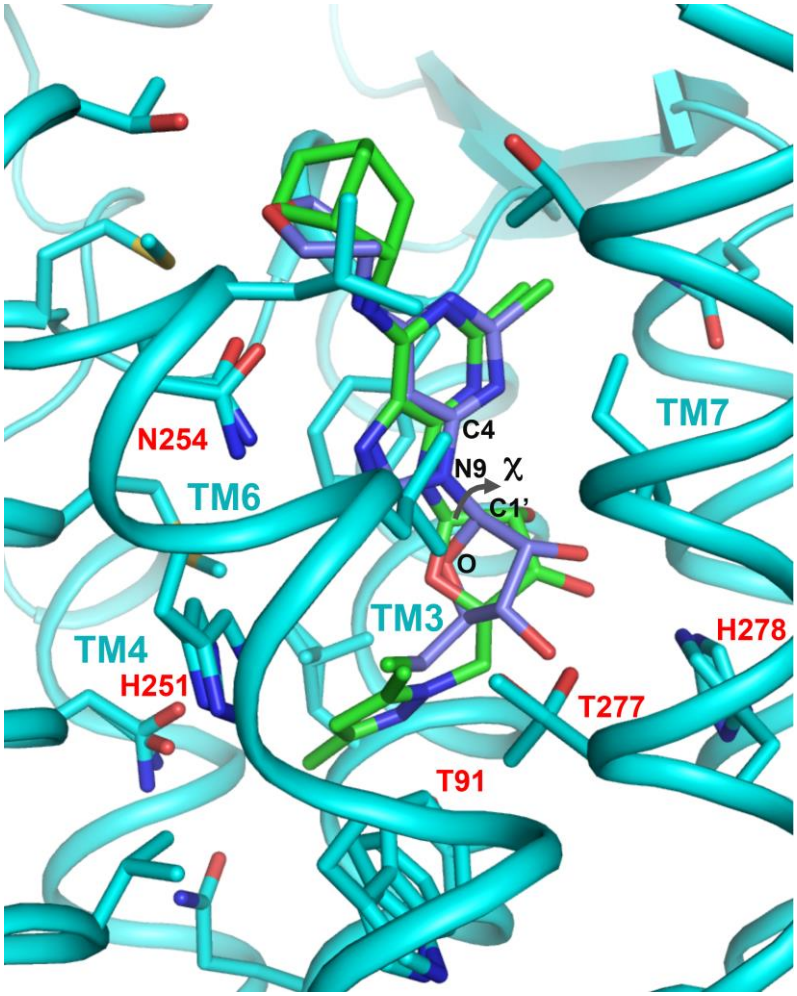

Figure 2. Overlay of the binding modes of **6** (slate carbons) and **12** (green carbons) at the binding pocket of hA_1AR. The glycosyl torsion angle χ (defined by O-C1'-N9-C4) is indicated. The amino acids important for ligand recognition ($T91^{3.36}$, $H251^{6.52}$, $N254^{6.55}$, $T277^{7.42}$, $H278^{7.43}$) are labeled in red. It can be seen the different orientation of the ribose moiety in the two adenosine derivatives.

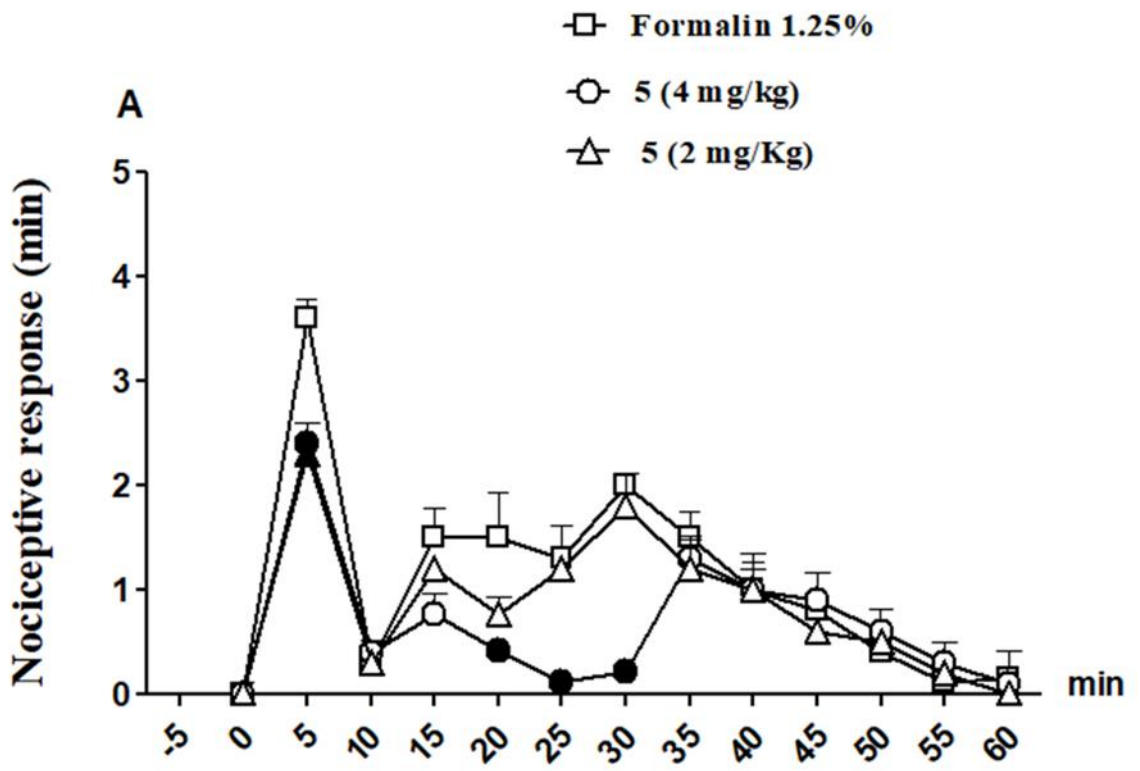
A
Formalin 1.25%
5 (4 mg/kg)
5 (2 mg/Kg)
Nociceptive response (min)
0
1
2
3
4
5
-5
0
5
10
15
20
25
30
35
40
45
50
55
60
min

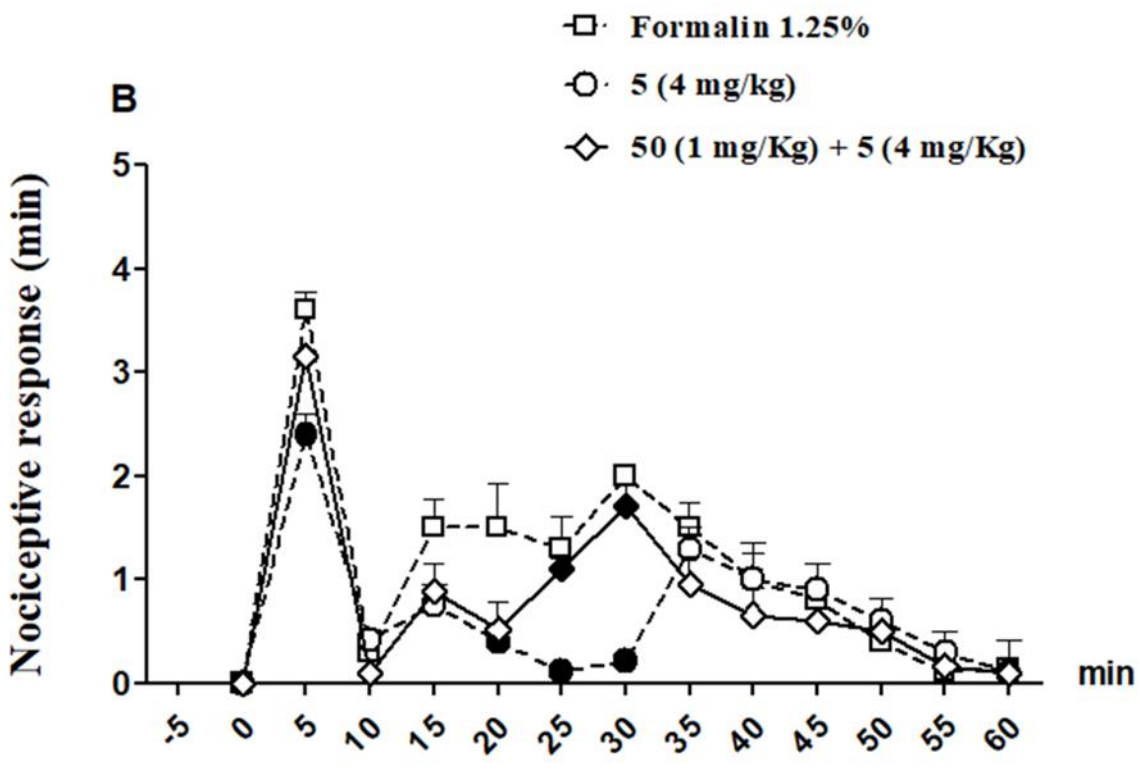
B
Formalin 1.25%
5 (4 mg/kg)
50 (1 mg/Kg) + 5 (4 mg/Kg)
Nociceptive response (min)
0
1
2
3
4
5
-5
0
5
10
15
20
25
30
35
40
45
50
55
60
min

Figure 3. Effect of subcutaneous formalin (1.25%, 30 μL) injections into the hind paw of mice on the time course of the nociceptive behaviors. Formalin was injected 10 min after the systemic administration of vehicle (0.9% NaCl, i.p.) or drugs. Part A shows the effects of the systemic administration of **5** (2 and 4 mg/kg, i.p.). Part B shows the effects of the systemic administration of **5** (4 mg/kg, i.p.) in combination with **50** (1 mg/kg, i.p.). Dotted lines indicate the data in Part A which are repeated in Part B. Recording of nociceptive behavior began immediately after the injection of formalin (time 0) and was continued for 60 min. Each point represents the total time of the nociceptive responses (mean (S.E.M.) of 8 mice per group, measured every 5 min. Full symbols indicate significant differences versus vehicle or versus drug alone. $P < 0.05$ was considered statistically significant.

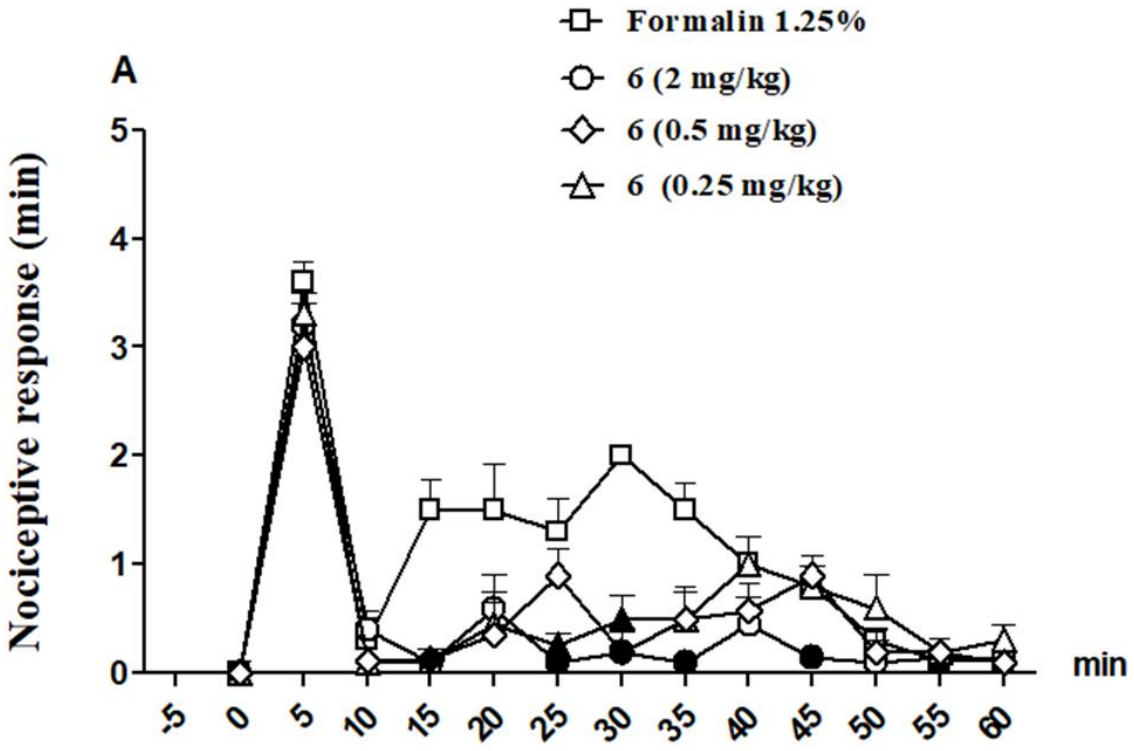
A
Formalin 1.25%
6 (2 mg/kg)
6 (0.5 mg/kg)
6 (0.25 mg/kg)
Nociceptive response (min)
0
1
2
3
4
5
-5
0
5
10
15
20
25
30
35
40
45
50
55
60
min

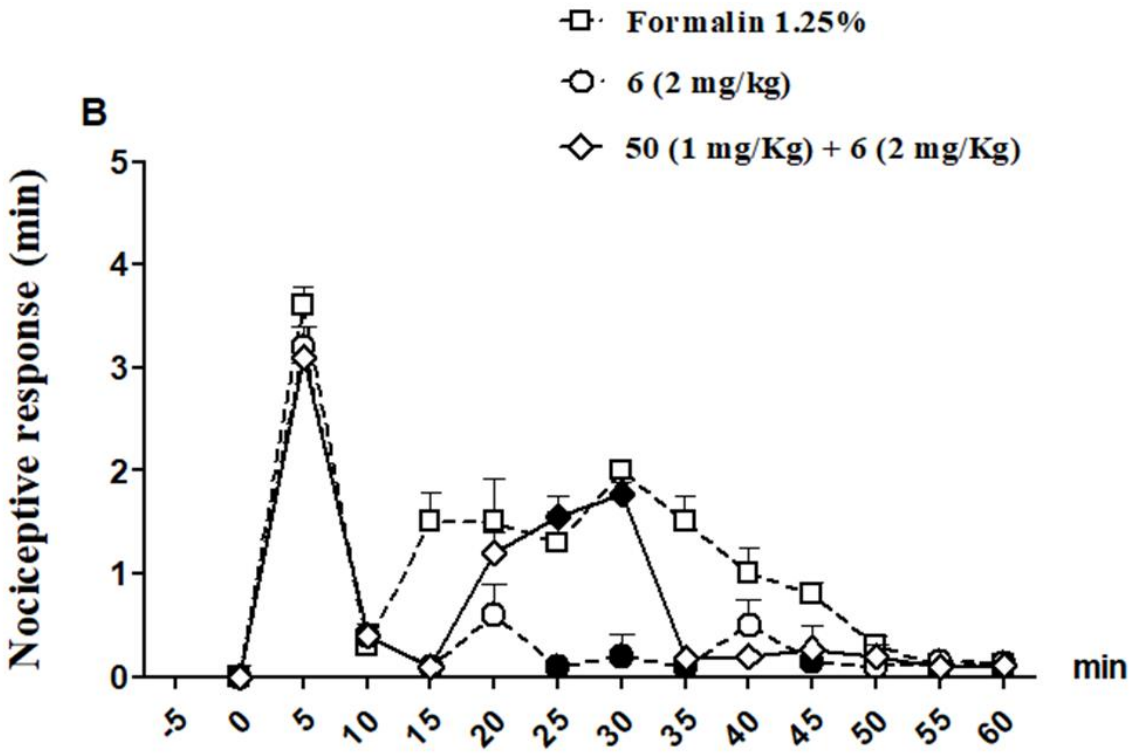
B
Formalin 1.25%
6 (2 mg/kg)
50 (1 mg/Kg) + 6 (2 mg/Kg)
Nociceptive response (min)
0
1
2
3
4
5
-5
0
5
10
15
20
25
30
35
40
45
50
55
60
min

Figure 4. Effect of subcutaneous formalin (1.25%, 30 μL) injections into the hind paw of mice on the time course of the nociceptive behaviors. Formalin was injected 10 min after the systemic administration of vehicle (0.9% NaCl, i.p.) or drugs. Part A shows the effects of the systemic administration of **6** (0.25, 0.5 and 2 mg/kg, i.p.). Part B shows the effects of the systemic administration of **6** (2 mg/kg, i.p.) in combination with **50** (1 mg/kg, i.p.). Dotted lines indicate the data in Part A which are repeated in Part B. Recording of nociceptive behavior began immediately after the injection of formalin (time 0) and was continued for 60 min. Each point represents the total time of the nociceptive responses (mean (S.E.M.) of 8 mice per group, measured every 5 min. Full symbols indicate significant differences versus vehicle or versus drug alone. $P < 0.05$ was considered statistically significant.

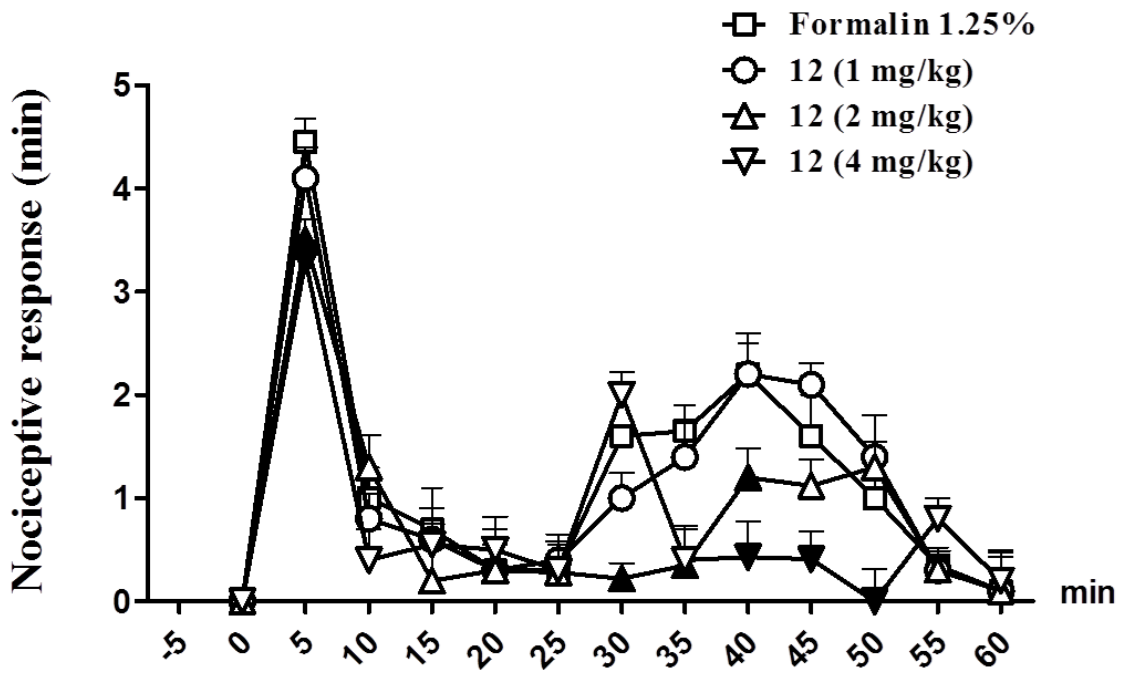

Figure 5. Effect of subcutaneous formalin (1.25%, 30 μL) injections into the hind paw of mice on the time course of the nociceptive behaviors. Formalin was injected 10 min after the systemic administration of vehicle (0.9% NaCl, i.p.) or drugs. Figure 3 shows the effects of the systemic administration of **12** (1, 2 and 4 mg/kg, i.p.). Recording of nociceptive behavior began immediately after the injection of formalin (time 0) and was continued for 60 min. Each point represents the total time of the nociceptive responses (mean (S.E.M.) of 8 mice per group, measured every 5 min. Full symbols indicate significant differences versus vehicle. $P < 0.05$ was considered statistically significant.

Table of Contents graphic